Contrib Mineral Petrol (2000) 139: 418–435

Roland Eichhorn · Georg Loth · Rudolf Höll
Fritz Finger · Andreas Schermaier · Allen Kennedy

Multistage Variscan magmatism in the central Tauern Window (Austria) unveiled by U/Pb SHRIMP zircon data

Received: 28 September 1999 / Accepted: 27 February 2000

Abstract U/Pb SHRIMP ages of nine Variscan leucocratic orthogneisses from the central Tauern Window (Austria) reveal three distinct pulses of magmatism in Early Carboniferous (Visean), Late Carboniferous (Stephanian) and Early Permian, each involving granitoid intrusions and a contemporaneous opening of volcano-sedimentary basins. A similar relationship has been reported for the Carboniferous parts of the basement of the Alps further to the west, e.g. the "External massifs" in Switzerland. After the intrusion of subduction-related, volcanic-arc granitoids (374 ± 10 Ma; Zwölferkogel gneiss), collisional intrusive-granitic, anatectic and extrusive-rhyolitic/dacitic rocks were produced over a short interval at ca. 340 Ma (Augengneiss of Felbertauern: 340 ± 4 Ma, Hochweißenfeld gneiss: 342 ± 5 Ma, Falkenbachlappen gneiss: 343 ± 6 Ma). This Early Carboniferous magmatism, which produced relatively small volumes of melt, can be attributed to the amalgamation of the Gondwana-derived "Tauern Window" terrane with Laurussia–Avalonia. Probably due to the oblique nature of the collision, transtensional phenomena (i.e. volcano-sedimentary troughs and high-level intrusives) and transpressional regimes (i.e. regional metamorphism and stacked nappes with anatexis next to thrust planes) evolved contemporaneously. The magmas are mainly of the high-K I-type and may have been generated during a short phase of decompressional melting of lithospheric mantle and lower crustal sources. In the Late Carboniferous, a second pulse of magmatism occurred, producing batholiths of calc-alkaline I-type granitoids (e.g. Venediger tonalite: 296 ± 4 Ma) and minor coeval bodies of felsic and intermediate volcanics (Heuschartenkopf gneiss: 299 ± 4 Ma, Peitingalm gneiss: 300 ± 5 Ma). Prior to this magmatism, several kilometres of upper crust must have been eroded, because volcano-sedimentary sequences hosting the Heuschartenkopf and Peitingalm gneisses rest unconformably on 340-Ma-old granitoids. The youngest (Permian) period of magma generation contains the intrusion of the S-type Granatspitz Central Gneiss at 271 ± 4 Ma and the extrusion of the rhyolitic Schönbachwald gneiss protolith at 279 ± 9 Ma. These magmatic rocks may have been associated with local extension along continental wrench zones through the Variscan orogenic crust or with a Permian rifting event. The Permian and the above-mentioned Late Carboniferous volcano-sedimentary sequences were probably deposited in intra-continental graben structures, which survived post-Variscan uplift and Alpine compressional tectonics.

R. Eichhorn (✉)
Bayerisches Geologisches Landesamt, Heßstr. 128,
80797 Munich, Germany
e-mail: roland.eichhorn@gla.bayern.de
Tel.: + 49-89-92142787; Fax: + 49-89-92142647

G. Loth · R. Höll
Institut für Allgemeine und Angewandte Geologie, Luisenstr. 37,
80333 Munich, Germany

F. Finger · A. Schermaier
Institut für Mineralogie, Hellbrunnerstr. 34, 5020 Salzburg, Austria

A. Kennedy
Curtin University of Technology, G.P.O. Box U 1987,
Perth 6001, Australia

Editorial responsibility: J. Hoefs

Introduction

Central Gneiss masses ("Zentralgneise") represent a major fraction of the rock lithologies of the Tauern Window area (Central Alps, Austria). They occur as large plutons and sheets produced by Early Alpine nappe-thrusting. Moreover, they display differences in their petrographic and geochemical compositions. Age dating, predominantly by the Rb–Sr whole rock method, confirmed a Variscan age of their protoliths (data compilation in Finger et al. 1993). However, the possibility of isotopic disturbance and resetting in this system have hampered modelling of the Variscan evolution in the Tauern Window.

More precise data have been published outside the Tauern Window (data compilation in Raumer 1998) with the Variscan orogen having been identified in various outcropping basement units of the Alps exposed by the collision of Gondwana and Laurussia. Voluminous granitoid plutons intruded within (nowadays) polymetamorphic pre-Variscan lithologies, and volcano-sedimentary troughs formed. These troughs of Late Carboniferous to Permian age are often considered to be successor basins of older basins containing Early Carboniferous sediments and volcanics (Fig. 1a, b). For example, an older sequence of clastic sediments and pyroclastic tuffs formed between 345 and 335 Ma in a transtensional basin now exposed in the External domain; subsequently, it was covered unconformably by ignimbrites, tuffs and rhyolites at 303–298 Ma (Schaltegger and Corfu 1995). This volcanism is coeval with voluminous intermediate to acid plutonism, occurring in several pulses in Early Carboniferous (342–330 Ma), Late Carboniferous (310–295 Ma) and Early Permian (280–270 Ma) times (Schaltegger and Corfu 1992, 1995; Schaltegger 1997).

It has been speculated that the basement units of the External domain have their eastern continuation in equivalent rock units of the Tauern Window area (Schumacher and Laubscher 1996; Raumer 1998). Yet, this correlation has been hampered by the scarcity of precise age data from the Tauern Window. In particular, sufficient reliable age data have so far not been available for the volcano-sedimentary lithologies preserved in synforms. Thus, the aim of this study is to unravel the period(s) of volcano-sedimentary deposition at surface and of the magmatic processes at deeper structural levels in the central Tauern Window using U/Pb SHRIMP ages for zircons from nine Variscan leucocratic gneisses.

Geology and sample selection

The central Tauern Window consists of a pre-Variscan basement, which is intruded by Variscan granitoids and locally covered by Variscan volcanics and sediments. The basement consists of (metamorphosed) Cambro-Ordovician magmatites and sediments of an active continental margin (Habach Group; arc and fore-arc lithologies) and ensialic back-arc lithologies (Stubach Group and equivalents in the Old Gneiss Series) (Eichhorn et al. 1999).

Variscan granitoids in the western and central Tauern Window are mainly represented by Central Gneiss bodies. Besides the more voluminous Central Gneiss plutons and their frequently aplitic injections into roof

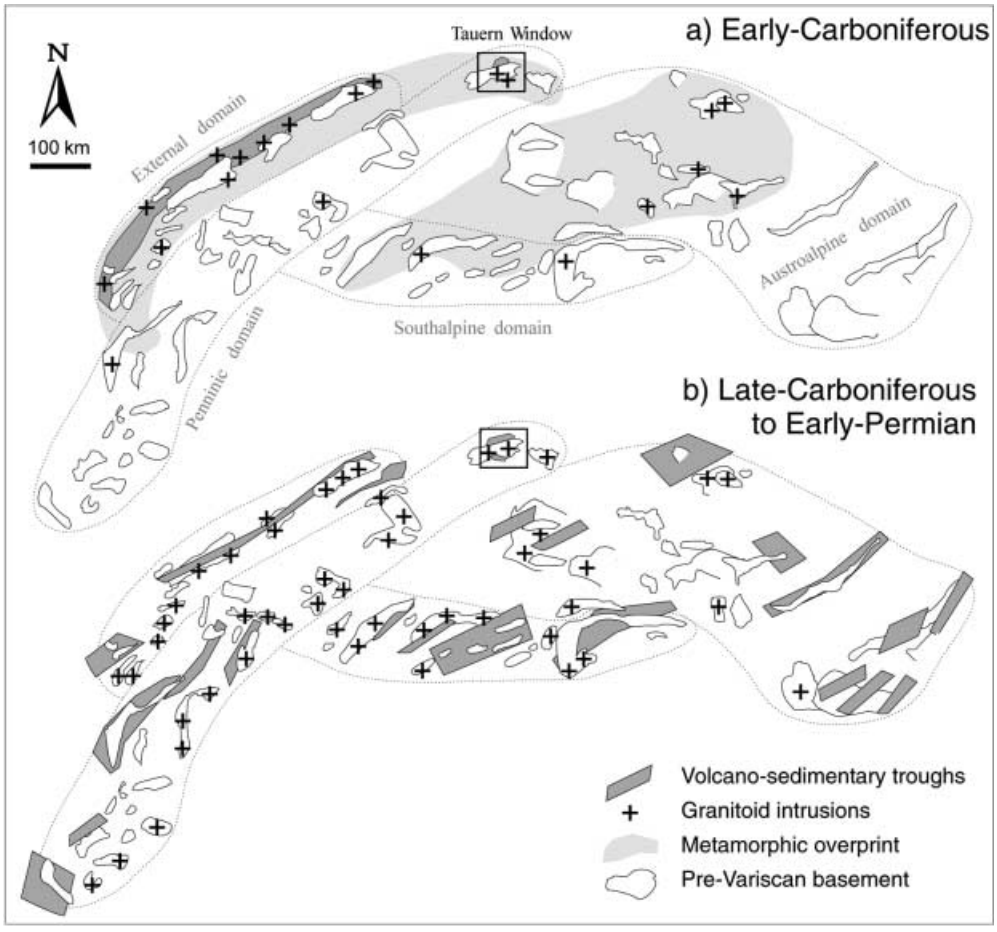

Fig. 1 Pre-Variscan basement areas, Variscan volcano-sedimentary troughs, regions of metamorphic overprint and granitoid intrusions in the present Alps. Basement areas have been detected in all four domains (External, Penninic, Austroalpine, Southalpine) of the Alpine orogeny. Both maps use a Permian reconstruction for better comparison of the relative positions of Early Carboniferous **a** and Late Carboniferous to Early Permian **b** volcano-sedimentary troughs and granitoid intrusions, although the reconstruction is not valid for Early Carboniferous times (cf. Fig. 9). Contours of the basement areas represent the present-day state, after Alpine shortening, and a more realistic pre-Permian reconstruction should take account of 30–60% of Alpine shortening of most areas (modified after Raumer 1998; our data already included). Framed area of the Tauern Window is enlarged in Fig. 2

rocks, thin elongate gneiss lamellae and minor intrusive gneiss bodies occur. Nappes with the Ahorn, the Granatspitz, the Tux, the Zillertal and the Venediger batholiths were stacked during Early Alpine compressional tectonics (Lammerer and Weger 1998; Figs. 2, 3). The gneiss lamella of the Tux nappe in the central Tauern Window (i.e. the Augengneiss of Felbertauern; Frasl and Frank 1966) probably marks the base of such a nappe sole thrust, but still displays an intrusive-magmatic texture. In contrast, the gneiss lamellae of the Venediger nappe (Hochweißenfeld gneiss; Fuchs 1958; Knorrkogel gneiss; Tollmann 1975) are interpreted as Early Carboniferous "in situ" anatexites and deep-seated granitoids adjacent to Variscan nappe-internal branch thrusts (Finger et al. 1993).

The spatial, temporal and geochemical evolution of the Variscan granitoids during the Variscan orogeny has been studied by various authors (Finger and Steyrer 1988, 1990; Finger et al. 1993, 1997; Schermaier 1993; Winkler 1996). However, their evolutionary models are based on limited age data: Finger et al. (1993, 1997) and Schermaier (1993) proposed that the Central Gneisses include at least three generations of Variscan granitoids: It has been inferred that Early Carboniferous high-K, biotite-rich I-type intrusive and anatectic melts (e.g. Hochweißenfeld gneiss, Knorrkogel gneiss) represent the oldest granitoids. This group was intruded after a period of significant uplift by voluminous Late Carboniferous calc-alkaline I-type granitoids, comprising the Zillertal–

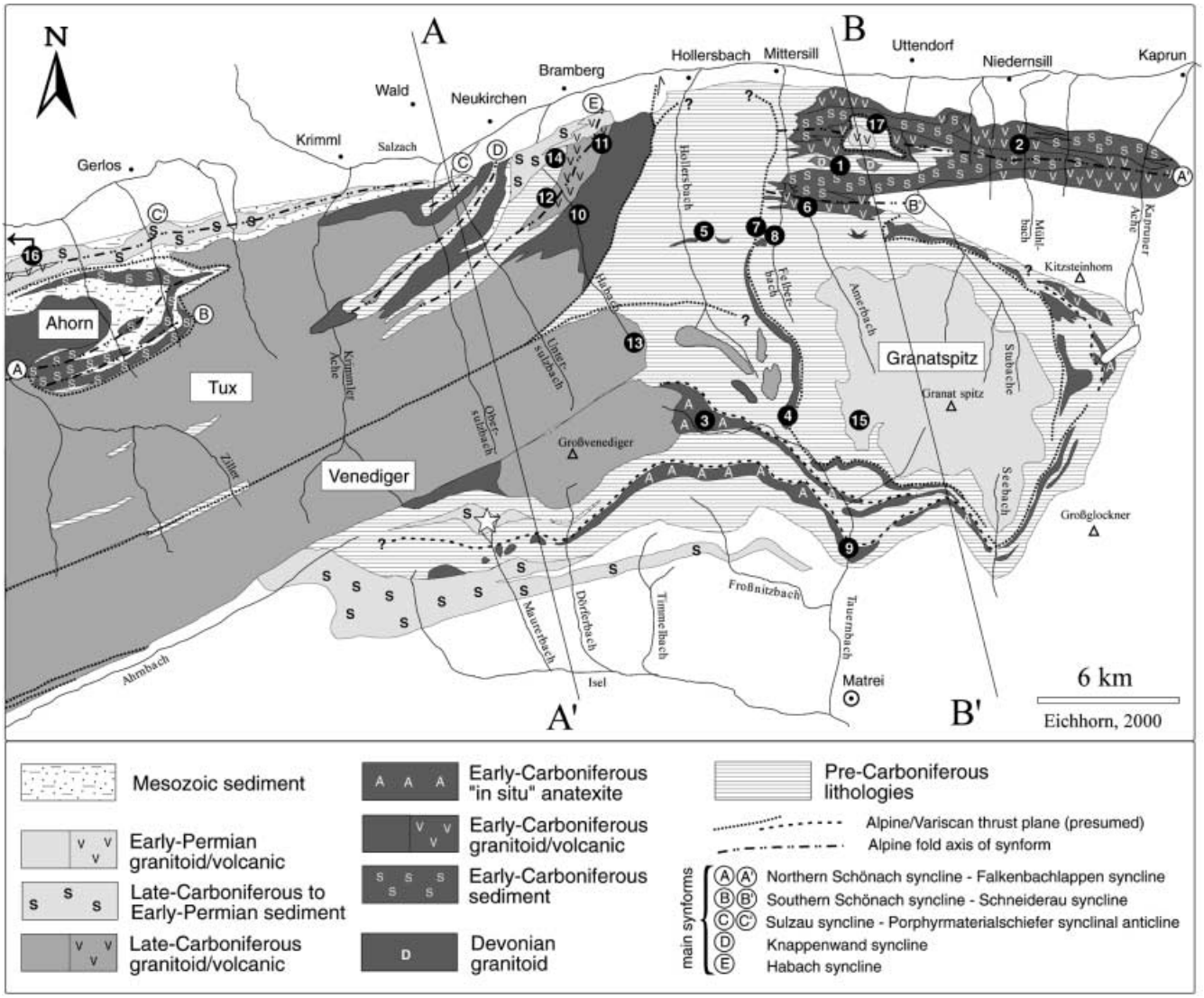

Fig. 2 Geological sketch-map of the western and central Tauern Window [modified after Schmidegg (1961), Raith et al. (1980), Lammerer (1986), Finger et al. (1993), Kupferschmied (1993, 1994), Oehlke et al. (1993), Schermaier (1993), Kupferschmied and Höll (1994), Kupferschmied et al. (1994), Lammerer and Weger (1998), Weger (1998), and unpublished maps of several diploma theses at the Institut für Allgemeine und Angewandte Geologie; Ludwig-Maximilians-Universität München]. *Lines A–A′* and *B–B′* indicate the positions of geological cross sections in Fig. 3. *Numbers* indicate approximate sample localities for the age data compiled in Table 1. The Permo-Carboniferous plant fossil find is indicated by a *star*. Our age results, the published age data of Table 1, and the relative intrusion and deposition ages as indicated by field observations have been integrated into the sketch-map

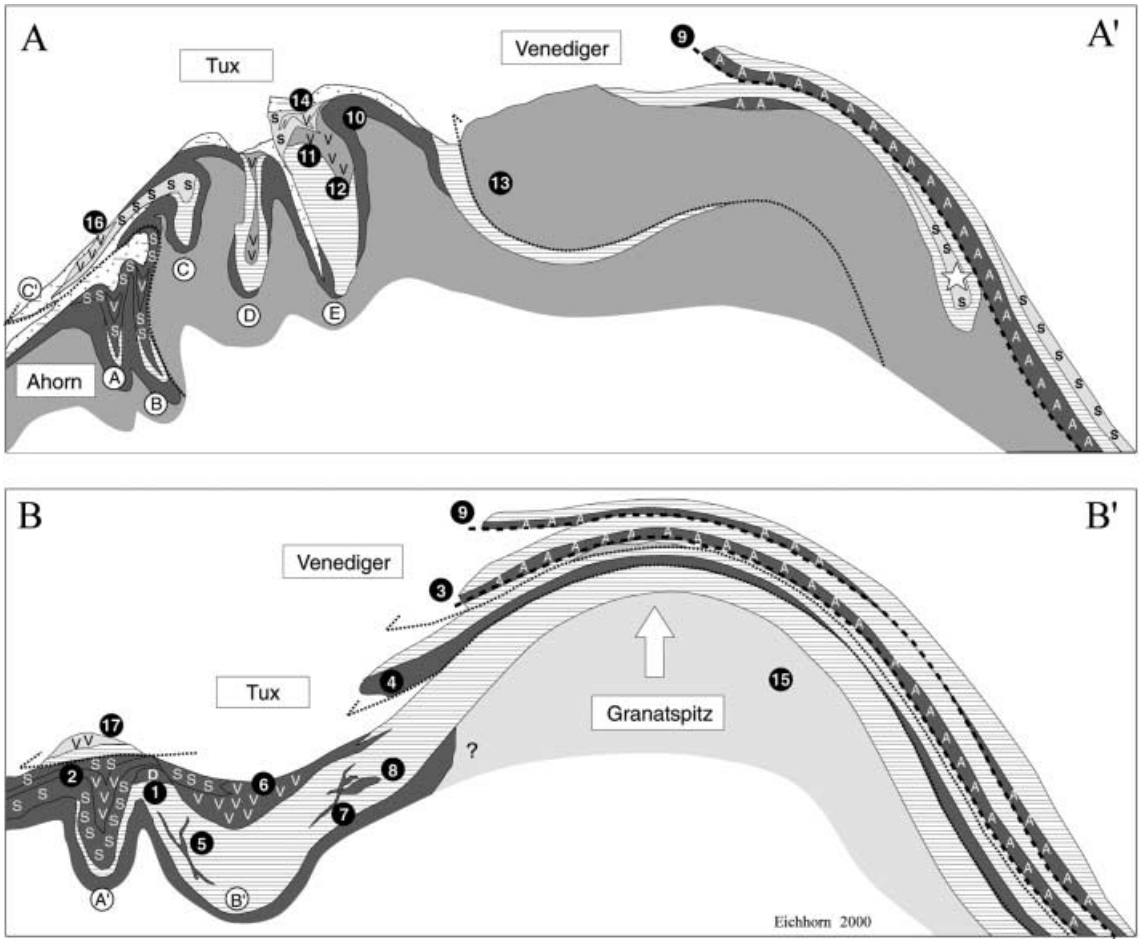

Fig. 3 Geological cross sections through the western and central Tauern Window in down-plunge view modified after Schmidegg (1961), Raith et al. (1980), Lammerer (1986), Kupferschmied (1993, 1994), Oehlke et al. (1993), Kupferschmied and Höll (1994), Kupferschmied et al. (1994), Lammerer and Weger (1998), Weger (1998) and our unpublished observations. The present erosion level is not indicated. Not to scale. For legend see Fig. 2

Venediger tonalites, granodiorites and granites and the Tux granodiorites and granites (''Augen- and Flasergneisses''). A-type granites such as the Felbertauern Augengneiss are presumed to be of Permian age. The S-type Granatspitz Central Gneiss is petrographically and geochemically unique in the Tauern Window area, and has been correlated with the oldest stage of Variscan granitoids (Finger et al. 1993, 1997; Schermaier 1993).

For this study, we have sampled Variscan granitoids covering all the presumed three stages of Variscan granitoids: Hochweißenfeld gneiss, Granatspitz Central Gneiss, Venediger Central Gneiss, and Augengneiss of Felbertauern (Table 1). Furthermore, a granodioritic intrusion into the pre-Variscan basement of the Stubach Group (Zwölferkogel gneiss) has been investigated. Based on field and petrographic evidence, this rock may represent one of the earliest intrusives of the Variscan orogeny.

Variscan volcanics and sediments have been identified in the western Tauern Window outcrops that survived post-Variscan uplift, Alpine compressional tectonics and erosion in synforms. The Tux nappe includes a ''Post-Variscan Transgression Series'', which discordantly overlies a pre-Carboniferous basement in the Greiner and Schönbichler synclines. Besides conglomeratic sediments, a thin rhyolitic layer of unknown age occurs (Lammerer 1986). A similar sedimentary unit with rhyolitic tuffaceous conglomerates is present in the Southern and Northern Schönach syncline; there, the pre-Carboniferous basement lithologies are reduced to small lenses of graphitic phyllites (Sengl 1991) (Figs. 2, 3). The ''Porphyrmaterialschiefer Series'' preserved in the Tux nappe at the northern margin of the Tauern Window resembles the sediments of the two Schönach synclines (Thiele 1974; Beil-Grzegorczyk 1988). Concordant layers of leucocratic meta-volcanics from that ''series'' have been dated at 284 + 2/−3 Ma (Söllner et al. 1991; Table 1).

In the central Tauern Window, the existence of similar relics of volcano-sedimentary basins has been locally assumed, although it is still unproven: The Venediger nappe displays a ''Micaschist Unit'' at the southern Tauern Window margin. This unit is partially folded into pre-Variscan basement rocks of the Old Gneiss Series (Schmidegg 1961; Raith et al. 1980). From that unit, a graphite schist lamella in the Maurer valley yielded a single ''pteridophyll'' leaf fragment of

most probably Late Carboniferous to Early Permian age (Franz et al. 1991). Early Carboniferous ages have been reported from the Habach valley of the Tux nappe (334 + 39/−25 Ma; Vavra 1989; Vavra and Hansen 1991) and from the Amer and Hollersbach valleys of the Granatspitz nappe (352 ± 12 and 355 ± 5 Ma respectively; Peindl and Höck 1993; Table 1). However, the Habach valley sample [a meta-rhyolite according to Vavra (1989) and Vavra and Hansen (1991)] has been later reinterpreted as a Central Gneiss variant (A-type meta-granite) by Kupferschmied (1994) and Kupferschmied and Höll (1994) due to field mapping and geochemical criteria, and by Schermaier (1993) and Winkler (1996) due to zircontypological and geochemical studies. The latter author inferred that this gneiss type is unique in the central and western Tauern Window, resembling the Augengneiss of Felbertauern, only. The Hollersbach valley sample is derived from a tonalitic dyke according to Peindl and Höck (1993), and not from a concordant meta-volcanic layer. The Amer valley sample gave a concordant age of 352 ± 12 Ma; however, besides this brief information in an abstract, further data and possible implications are still unpublished. However, this is so far the only age that points to the existence of Variscan volcanics in the central Tauern Window. In the absence of geochronological data, earlier authors attributed the intermediate to leucocratic meta-volcanics and meta-sediments to the pre-Variscan Habach Group (Frasl 1958; Höll 1975; Steyrer 1982, 1983; Steyrer and Höck 1985). Only recently, erosional unconformities between Habach Group lithologies and overlying (Variscan?) meta-volcanics and meta-sediments have been reported from the Habach syncline (Kupferschmied 1994; Kupferschmied and Höll 1994) and the Schneiderau syncline (Kraiger 1989).

The Habach syncline at the northern front of the Tux nappe consists of graphite-rich phyllites as well as coarse- and fine-grained amphibolites and greenschists of the pre-Variscan Habach Group, which have been intruded by an A-type microgranite at 334 + 39/−25 Ma (Vavra 1989; Vavra and Hansen 1991). An angular unconformity separates these lithologies from overlying felsic tuffs and tuffites intercalated with enclaves of mafic lapilli-tuffs and tuffaceous breccias and overlain by intermediate, andesitic to dacitic lavas, tuffs and tuffites. The poorly sorted clasts of the pyroclastics suggest a site rather proximal to a volcanic centre (Kupferschmied 1994). More distant, muscovite- and carbonate-rich micaschists and phyllites rest unconformably on Habach Group rocks. The erosional unconformity is marked by a "black schist" horizon overlain by light-coloured micaschists and phyllites (Kupferschmied 1994; Kupferschmied and Höll 1994).

We sampled a felsic rhyolitic tuff (Heuschartenkopf gneiss) and an intermediate dacitic lava (Peitingalm gneiss), as well as a small, concordant layer of a further rhyolitic tuff adjacent to the base of the "black schist" horizon in the light-coloured micaschists and phyllites (Schönbachwald gneiss). Furthermore, a rhyodacitic lava (Falkenbachlappen gneiss) overlain by micaschists and phyllites from the northern front of the Granatspitz nappe has been investigated.

Materials and methods

The samples comprised 10 to 40 kg of fresh material. Mineral fractions for isotopic analyses were processed through conventional mineral separation techniques, including a Wilfley table, heavy liquids and the Frantz isodynamic separator. Final mineral separates consisted of hand-picked, top-quality zircon grains, characterized by homogeneity, transparency, colour and fluorescence.

Zircon grains from the sample and a zircon standard are mounted and polished in a 24-mm-diameter epoxy disc and gold coated. The zircons are then photographed, examined by cathodoluminescence (CL) imaging and analysed using the SHRIMP II ion microprobe. During data reduction, correction for common Pb in the zircon uses the methods of Compston et al. (1984). The calculation of $^{206}Pb/^{238}U$ ages is based upon the assumption that the bias of the measured $^{206}Pb^{+}/^{238}U^{+}$ ratio relative to the true ratio can be described by the same power law relationship (Claoue-Long et al. 1995) between $^{206}Pb^{+}/^{238}U^{+}$ and UO^{+}/U^{+} for both the CZ3 standard zircon (Pidgeon 1997) and the unknown zircon analysis. The uncertainty of the $^{206}Pb/^{238}U$ age of the unknown zircon includes the uncertainty of the $^{206}Pb^{+}/^{238}U^{+}$ ratio of the standard. For this reason, approximately twice the number of "standard" analyses are interspersed between "unknowns" analyses in any analytical session. Reproducibility for the "standard" Pb/U ratio ranged between ±1.05% and ±2.22% for the six SHRIMP sessions required to analyse the samples. The concentrations of U, Th and Pb are calculated using a similar approach to that used for the calculation of U/Pb ratios with the unknown referenced to the standard with known U, Th and Pb abundances (Compston et al. 1984; Claoue-Long et al. 1995; Williams et al. 1996).

The zircons were examined with a Zeiss DSM 960A scanning electron microscope (SEM) at the Institut für Allgemeine und Angewandte Geologie, University of Munich, and with a JEOL 6400 at the Electron Microscopic Centre, University of Western Australia in Perth in back-scattered electron (BSE) and cathodoluminescence (CL) mode on polished and gold- or carbon-coated grain mounts for internal structures.

Errors cited for individual analyses include errors from counting statistics, the common-Pb correction and the U/Pb calibration error based on reproducibility of U/Pb measurements of the standard. They are at the 1σ level, whereas weighted mean values given on pooled analyses ($\chi^2 \approx 1$) are at the 2σ level (95% confidence level). Error polygons shown in Figs. 5, 6, 7 and 8 are at the 1σ level. The $^{206}Pb/^{238}U$ error is generally the smallest error, because $^{206}Pb/^{238}U$ dates for SHRIMP analyses of Proterozoic to Paleozoic zircons are more precise than $^{207}Pb/^{235}U$ and $^{207}Pb/^{206}Pb$ dates, due to the lower abundance of ^{207}Pb as compared with ^{206}Pb in such zircons. Decay constants used are those recommended by IUGS (Steiger and Jäger 1977). Upper intercept age calculations were calculated after Ludwig (1991). The terminology of periods and epochs quoted herein follows the chronostratigraphic time scale of Gradstein and Ogg (1996).

Results and interpretation

CL images of some of the investigated zircons are given in Fig. 4. Geochemical descriptions and further references are compiled in Table 1; U/Pb data in Table 2. Results are grouped from oldest to youngest and depicted in Figs. 5, 6, 7 and 8.

Table 1 Compilation of U/Pb zircon data from Variscan magmatites of the central Tauern Window

No.	Type	Name, location	Geochemistry	Recent geochemical references	U/Pb (Ma)	U/Pb reference with method applied
Devonian (Givetian)						
1	Plutonic	Zwölferkogel gneiss, Zwölferzug near Zwölferkogel, eastern slope of Felber valley	Medium- to high-K (calc-alkaline) VAG, I-type granodiorite	Loth and Höll (1996)	374 ± 10	This work, SHRIMP, concordant age
Early Carboniferous (Visean)						
2	Volcanic lava	Falkenbachlappen gneiss, western slope of Mühlbach valley (2038 m a.s.l.)	Medium-K (calc-alkaline) VAG, I-type rhyodacite	Jünger et al. (1999)	343 ± 6	This work, SHRIMP, concordant age
3	"In situ" anatectic	Hochweißenfeld gneiss, south of the Abretterkopf at Sandeben	High-K (shoshonite) VAG, I-type granite	Schermaier (1991, 1993), Finger et al. (1993)	342 ± 5	This work, SHRIMP, concordant age
4	Plutonic	Augengneiss of Felbertauern, south- western flank of the Meßelingkogel at 2220 m a.s.l.	High-K (shoshonite) VAG, A-type granite	Finger et al. (1993), Schermaier (1993), Gritz (1996), Winkler (1996)	340 ± 4	This work, SHRIMP, concordant age
5	Sub-volcanic	Tonalitic dyke, Hollersbach valley about 6 km south of Hollersbach	I-type tonalite	–	355 ± 5	Peindl and Höck (1993), zircon evaporation, Kober method (abstr)
6	Volcanic lava/tuff ?	Albite–epidote gneiss, Amer valley near junction with Felber valley	High-K (calc-alkaline) VAG, I-type rhyolite	Höck et al. (1993)	352 ± 12	Peindl and Höck (1993), conventional dilution, upper intercept (abstr)
7	Sub-volcanic	Dacitic dyke, Felber valley, western slope tungsten deposit (1050 m level)	High-K (calc-alkaline) VAG (±syn-COLG), I-type granodiorite	Teipel and Höll (2000)	340 ± 5	Eichhorn et al. (1999), SHRIMP, concordant age
8	Sub-volcanic	K1–K3 gneiss, Felber valley, western slope tungsten deposit	High-K (calc-alkaline) WPG (±syn-COLG), A-type granite	Finger et al. (1985), Eichhorn (1995), Eichhorn et al. (1997)	336 ± 19	Eichhorn et al. (1995), conventional dilution, upper intercept
9	"In situ" anatectic	Knorrkogelgneiss, Matreier Tauern valley, Raneburg	High-K (calc-alkaline) VAG, I-type granite	Finger et al. (1993), Schermaier (1993), Gritz (1996)	334 ± 8	Finger and Quadt (1993), conventional dilution, upper intercept (abstr)
10	Plutonic	K-feldspar–plagioclase gneiss, near bridge over Habach river at 1107 m a.s.l.	High-K (calc-alkaline) VAG (±WPG), A-type granite	Vavra (1989), Schermaier (1993), Kupferschmied (1994)	334 + 39/−25	Vavra and Hansen (1991), conventional dilution, upper intercept
Late Carboniferous (Stephanian)						
11	Volcanic tuff	Peitingalm gneiss, near forest lane (1095 m a.s.l.) in the Habach valley	Medium- to high-K (calc-alkaline) VAG, I-type dacite	Steyrer (1982), Vavra (1989), Kupferschmied (1994)	300 ± 5	This work, SHRIMP, concordant age
12	Volcanic tuff	Heuschartenkopf gneiss, forest lane west of Wennser Bach (1200 m a.s.l.), Habach valley	High-K (calc-alkaline) VAG/ WPG, I-type rhyolite	Steyrer (1982), Kupferschmied and Höll (1994)	299 ± 4	This work, SHRIMP, concordant age
13	Plutonic	Venediger Central Gneiss, eastern slope of the Habach valley at 1960 m a.s.l.	Low-K (calc-alkaline) VAG, I-type tonalite	Finger et al. (1993), Schermaier (1993), Winkler (1996)	296 ± 4	This work, SHRIMP, concordant age

Permian						
14	Volcanic tuff	Schönbachwald gneiss, about 2000 m south of Habach in the Habach syncline	Medium-K (calc-alkaline) VAG, I-type rhyolite	Kupferschmied (1994), Kupferschmied and Höll (1994)	279 ± 7	This work, SHRIMP, concordant age
15	Plutonic	Granatspitz Central Gneiss, about 100 m east of Schwarzer See at 2400 m a.s.l.	High-K (calc-alkaline) syn-COLG, S-type granite	Finger and Steyrer (1988), Finger et al. (1993), Winkler (1996)	271 ± 4	This work, SHRIMP, slightly discordant age
16	Volcanic tuff	Porphyroid gneiss, from the Tuxer valley near Mayrhofen between Finkenberg and Astegg	Rhyolite	Beil (1986), Beil-Grzegorczyk (1988)	284 + 2/−3	Söllner et al. (1991), conventional dilution, lower (!) intercept
17	Volcanic tuff/lava ?	Porphyroid gneiss of the Sturmmannseck, western slope of Stubach valley	Medium-K (calc-alkaline) post-COLG, S-type rhyolite	Loth and Höll (1996)	283 ± 11	Loth et al. (1997), SHRIMP, concordant age

Zwölferkogel gneiss (1; intrusive granodiorite)

All eight analyses plot analytically concordant with no excess scatter (Fig. 5). The identical mean $^{206}Pb/^{238}U$ and $^{207}Pb/^{235}U$ ages of 374 ± 10 Ma ($\chi^2 = 0.88$ and 0.95 respectively) indicate the crystallization age of the granodiorite.

Falkenbachlappen gneiss (2; rhyodacitic lava)

All 11 analyses from centre and rim zones form a single, coherent population plotting analytically concordant with some excess scatter (Fig. 6a). The mean $^{206}Pb/^{238}U$ age of 343 ± 6 Ma ($\chi^2 = 3.75$) and the mean $^{207}Pb/^{235}U$ age of 349 ± 6 Ma ($\chi^2 = 1.20$) may indicate the crystallization age of the rhyodacite.

Hochweißenfeld gneiss (3; "in situ" anatectic granite)

Fifteen analyses from all zones of the zircons form a single concordant population with a mean $^{206}Pb/^{238}U$ age of 342 ± 5 Ma ($\chi^2 = 3.23$) and a mean $^{207}Pb/^{235}U$ age of 343 ± 5 Ma ($\chi^2 = 2.42$) (Fig. 6b). Only one spot on grain 10 is omitted from the calculation due to its slight discordancy and unusually low U content of 234 ppm compared with the normal range of 1028–3137 ppm U.

Augengneiss of Felbertauern (4; intrusive granite)

Thirteen analyses from the various zones form a single concordant population with no excess scatter. They yield mean U/Pb ratios equivalent to a $^{206}Pb/^{238}U$ age of 340 ± 4 Ma ($\chi^2 = 0.83$) and a $^{207}Pb/^{235}U$ age of 341 ± 4 Ma ($\chi^2 = 0.72$) (Fig. 6c). The 340 Ma age is interpreted as the crystallization age of the granitic precursor of the Augengneiss of Felbertauern. Four analyses are discordant with lower U/Pb ratios due to SHRIMP spots on highly metamict zones (spot 1 r and 12 with 7435 ppm U and 5273 ppm U respectively) or on cracks (spot 6), which caused rejuvenated ages due to Pb loss. Such cracks have obviously been used as pathways for fluids, which leached the more easily solvable radiogenic Pb compared to common Pb. This is documented in the two SHRIMP analyses 6 and 6c, which have been placed in the same growth zone, yet one spot is on a diffusion channel (visible in the CL image), the other on an undisturbed area (Fig. 4b, grain 6). As presumed, the analyses on the crack yielded significantly younger U/Pb ages than the one from the undisturbed region.

Peitingalm gneiss (11; dacitic tuff)

Seventeen grains have been analysed. Apart from analyses 1, 10, 12 and 9, the remaining 13 analyses from

Table 2 U/Pb data. In grain column: spot positions are *c* centre, *r* rim, or intermediate between *c* and *r* (no suffix)

Grain	$U_{(ppm)}$	$Th_{(ppm)}$	$Pb_{(ppm)}$	Calculated ratios						Calculated ages in Ma ($\pm 1\ \sigma$)					
				$^{206}Pb/^{238}U$	($\pm 1\ \sigma$)	$^{207}Pb/^{235}U$	($\pm 1\sigma$)	$^{207}Pb/^{206}Pb$	($\pm 1\ \sigma$)	$^{206}Pb/^{238}U$		$^{207}Pb/^{235}U$		$^{207}Pb/^{206}Pb$	
Zwölferkogel gneiss (1; intrusive granodiorite)															
1	391	1	24	0.061168	0.001654	0.455813	0.015479	0.054045	0.000943	383	10	381	11	373	39
2	495	2	27	0.057841	0.001565	0.430373	0.014366	0.053965	0.000888	362	10	363	10	370	37
3	1648	4	94	0.061761	0.001630	0.454573	0.012709	0.053381	0.000347	386	10	380	9	345	15
4	298	2	18	0.060110	0.001636	0.428494	0.015914	0.051701	0.001142	376	10	362	11	272	51
5	740	2	41	0.058529	0.001558	0.430806	0.012978	0.053384	0.000595	367	9	364	9	345	25
6	496	1	29	0.060337	0.001618	0.459555	0.014756	0.055240	0.000808	378	10	384	10	422	33
7	409	1	23	0.058093	0.001569	0.439251	0.014534	0.054839	0.000879	364	10	370	10	406	36
8	450	1	27	0.061633	0.001655	0.465832	0.014916	0.054817	0.000790	386	10	388	10	405	32
Falkenbachlappen gneiss (2; rhyodacitic lava)															
1c	222	84	13	0.056363	0.000776	0.440176	0.030298	0.056642	0.003724	353	5	370	21	478	146
1	321	155	19	0.054855	0.000684	0.424377	0.022735	0.056110	0.002837	344	4	359	16	457	112
2	280	113	15	0.053512	0.000672	0.398122	0.012747	0.053959	0.001507	336	4	340	9	369	63
3c	900	577	54	0.055447	0.000585	0.415769	0.006306	0.054384	0.000525	348	4	353	5	387	22
3	378	204	22	0.055173	0.000652	0.403838	0.012316	0.053085	0.001416	346	4	344	9	332	61
4c	890	643	52	0.052644	0.000560	0.389920	0.008782	0.053718	0.000997	331	3	334	6	359	42
4	300	127	17	0.055047	0.000691	0.420203	0.012883	0.055364	0.001464	345	4	356	9	427	59
5	279	141	16	0.054039	0.000718	0.401842	0.024107	0.053932	0.003067	339	4	343	17	368	128
6	283	163	16	0.053600	0.000696	0.397250	0.009594	0.053752	0.001011	337	4	340	7	361	42
7	427	260	25	0.054296	0.000663	0.400507	0.018494	0.053499	0.002302	341	4	342	13	350	97
8	808	859	55	0.056891	0.000591	0.419268	0.006103	0.053450	0.000481	357	4	356	4	348	20
Hochweißenfeld gneiss (3; "in situ" anatectic granite)															
1	1135	202	61	0.056302	0.000750	0.415702	0.006827	0.053550	0.000433	353	5	353	5	352	18
2	1531	254	82	0.056394	0.000745	0.419372	0.007039	0.053935	0.000477	354	5	356	5	368	20
3c	1122	389	61	0.054320	0.000721	0.398049	0.008495	0.052916	0.000787	341	4	337	6	325	32
3	1543	403	79	0.053952	0.000718	0.400489	0.007149	0.053735	0.000586	339	4	341	5	359	24
3r	1675	50	73	0.053148	0.000699	0.389455	0.006732	0.053110	0.000521	333	4	333	5	334	21
4	3137	408	168	0.056728	0.000735	0.419682	0.006208	0.053656	0.000306	356	4	356	4	357	13
5	1347	343	71	0.054012	0.000715	0.399232	0.007084	0.053609	0.000551	339	4	341	5	355	23
6	1352	349	73	0.055184	0.000731	0.405654	0.007236	0.053314	0.000555	346	4	346	5	342	24
6r	2913	641	147	0.053361	0.000694	0.384219	0.007357	0.052222	0.000654	335	4	330	5	295	29
7	2026	536	106	0.053447	0.000699	0.396949	0.007039	0.053865	0.000563	336	4	339	5	365	24
8	1910	406	101	0.054816	0.000718	0.404673	0.007005	0.053542	0.000525	344	4	345	5	352	22
9c	1028	103	53	0.055046	0.000737	0.407362	0.007258	0.053673	0.000547	345	5	347	5	357	23
9r	2905	208	143	0.053210	0.000691	0.389551	0.005791	0.053097	0.000308	334	4	334	4	333	13
10	243	77	14	0.051915	0.000800	0.388530	0.014768	0.054279	0.001784	326	5	333	11	383	74
11	1309	265	68	0.053656	0.000711	0.395349	0.007020	0.053440	0.000549	337	4	338	5	348	23
Augengneiss of Felbertauern (4; intrusive granite)															
1c	782	366	43	0.052550	0.000798	0.387631	0.009618	0.053499	0.000953	330	5	333	7	350	40
1	1511	373	81	0.054198	0.000801	0.396150	0.007580	0.053012	0.000554	340	5	339	6	329	24
1r	7435	584	225	0.032153	0.000466	0.234038	0.003727	0.052792	0.000265	204	3	214	3	320	11
2	768	160	42	0.055738	0.000845	0.412487	0.008972	0.053674	0.000742	350	5	351	6	357	31
3	888	205	47	0.053978	0.000813	0.409017	0.008485	0.054957	0.000688	339	5	348	6	410	28
4	1461	409	80	0.054911	0.000813	0.403496	0.007781	0.053294	0.000568	345	5	344	6	341	24
5	2571	619	136	0.054067	0.000791	0.394608	0.006866	0.052934	0.000411	339	5	338	5	326	18
6c	1765	704	95	0.053411	0.000790	0.389643	0.010958	0.052910	0.001172	335	5	334	8	325	50
6	1169	256	56	0.048934	0.000733	0.363331	0.009227	0.053851	0.001008	308	5	315	7	365	42
7	2897	604	151	0.053904	0.000787	0.397983	0.006773	0.053548	0.000380	338	5	340	5	352	16
8c	2023	863	113	0.054371	0.000800	0.397394	0.007597	0.053010	0.000557	341	5	340	6	329	24
8	1941	625	106	0.054460	0.000803	0.408630	0.008495	0.054419	0.000704	342	5	348	6	388	29
9	1388	395	69	0.048586	0.000725	0.355840	0.011089	0.053118	0.001357	306	4	309	8	334	58
10	1881	480	101	0.054305	0.000799	0.396421	0.007306	0.052944	0.000498	341	5	339	5	326	21
11	1784	425	93	0.053436	0.000788	0.391917	0.007592	0.053193	0.000578	336	5	336	6	337	25
12	5273	1047	205	0.040248	0.000585	0.298054	0.004876	0.053709	0.000318	254	4	265	4	359	13
13	1639	477	88	0.054374	0.000803	0.395608	0.007530	0.052768	0.000544	341	5	338	5	319	23
Peitingalm gneiss (11; dacitic tuff)															
1	476	160	22	0.046389	0.001006	0.354420	0.009079	0.055412	0.000621	292	6	308	7	429	25
2	845	195	38	0.046721	0.000995	0.330214	0.008491	0.051260	0.000615	294	6	290	6	253	28
3	1180	265	54	0.047221	0.001000	0.338982	0.007857	0.052064	0.000371	297	6	296	6	288	16
4c	791	162	37	0.048551	0.001035	0.350809	0.008936	0.052405	0.000604	306	6	305	7	303	26
4	791	177	35	0.046310	0.000988	0.342491	0.008228	0.053638	0.000466	292	6	299	6	356	20
5	448	97	21	0.049292	0.001070	0.357684	0.010201	0.052629	0.000842	310	7	310	8	313	36
6	1431	567	69	0.047827	0.001011	0.346271	0.007907	0.052510	0.000336	301	6	302	6	308	15
7	1139	344	52	0.045867	0.000973	0.332369	0.007759	0.052556	0.000392	289	6	291	6	310	17

Table 2 (*Contd.*)

Grain	$U_{(ppm)}$	$Th_{(ppm)}$	$Pb_{(ppm)}$	Calculated ratios						Calculated ages in Ma ($\pm 1\ \sigma$)					
				$^{206}Pb/^{238}U$	($\pm 1\ \sigma$)	$^{207}Pb/^{235}U$	($\pm 1\sigma$)	$^{207}Pb/^{206}Pb$	($\pm 1\ \sigma$)	$^{206}Pb/^{238}U$		$^{207}Pb/^{235}U$		$^{207}Pb/^{206}Pb$	
8	1542	364	72	0.048575	0.001026	0.354542	0.008044	0.052936	0.000322	306	6	308	6	326	14
9	1954	597	74	0.038498	0.000813	0.271189	0.007342	0.051089	0.000742	244	5	244	6	245	33
10	1820	433	76	0.042950	0.000906	0.304723	0.007706	0.051456	0.000594	271	6	270	6	261	27
11c	906	210	42	0.047912	0.001019	0.344964	0.008747	0.052219	0.000595	302	6	301	7	295	26
11	922	242	44	0.048246	0.001026	0.348928	0.008856	0.052453	0.000601	304	6	304	7	305	26
12	1120	377	6	0.041343	0.000879	0.296181	0.009557	0.051958	0.001130	261	5	263	7	284	50
13c	653	130	31	0.048804	0.001044	0.348622	0.009207	0.051808	0.000676	307	6	304	7	277	30
13	808	253	37	0.046208	0.000986	0.337381	0.008910	0.052955	0.000695	291	6	295	7	327	30
14	1152	253	54	0.048415	0.001025	0.347668	0.008462	0.052081	0.000502	305	6	303	6	289	22
Heuschartenkopf gneiss (12; rhyolitic tuff)															
1	607	320	31	0.048186	0.001078	0.338565	0.011657	0.050959	0.001199	303	7	296	9	239	54
2	501	161	24	0.047774	0.001075	0.358552	0.015349	0.054432	0.001835	301	7	311	11	389	76
3	674	365	35	0.048256	0.001077	0.342831	0.012327	0.051526	0.001316	304	7	299	9	264	59
4	1919	1842	97	0.043523	0.000957	0.315165	0.008060	0.052519	0.000556	275	6	278	6	308	24
5	638	286	32	0.048218	0.001078	0.344070	0.012163	0.051753	0.001280	304	7	300	9	275	57
6	444	182	21	0.045945	0.001040	0.316085	0.015238	0.049896	0.001988	290	6	279	12	190	92
7	567	296	28	0.047249	0.001058	0.338841	0.013066	0.052012	0.001493	298	7	296	10	286	66
8	742	399	36	0.046336	0.001032	0.340601	0.010712	0.053312	0.001045	292	6	298	8	342	44
9	547	260	27	0.047125	0.001056	0.328713	0.012820	0.050590	0.001479	297	7	289	10	222	68
10	509	201	25	0.047921	0.001074	0.350582	0.012687	0.053060	0.001366	302	7	305	10	331	58
11	1462	1294	80	0.047656	0.001050	0.338254	0.008928	0.051478	0.000620	300	6	296	7	262	28
12	156	70	7	0.045092	0.001099	0.335775	0.033828	0.054007	0.005118	284	7	294	26	371	215
13	119	50	6	0.048422	0.001209	0.360873	0.040075	0.054052	0.005682	305	7	313	30	373	238
14	312	155	16	0.047258	0.001083	0.327180	0.017588	0.050212	0.002302	298	7	287	13	205	106
15	203	122	11	0.047331	0.001114	0.331253	0.024626	0.050759	0.003433	298	7	291	19	230	155
Venediger Central Gneiss (13; intrusive tonalite)															
1c	523	202	25	0.047739	0.000680	0.353201	0.013589	0.053660	0.001824	301	4	307	10	357	77
1	2591	715	111	0.043690	0.000570	0.311465	0.005746	0.051704	0.000595	276	4	275	4	272	26
2	1713	397	82	0.049209	0.000648	0.360106	0.005659	0.053074	0.000377	310	4	312	4	332	16
3	2008	640	100	0.046060	0.000604	0.336566	0.006359	0.052996	0.000639	290	4	295	5	329	27
4	7149	1969	180	0.025519	0.000329	0.183314	0.003055	0.052100	0.000472	162	2	171	3	290	21
5	2143	585	92	0.043974	0.000576	0.314063	0.005619	0.051799	0.000552	277	4	277	4	277	24
5c	811	378	40	0.047628	0.000651	0.345166	0.009158	0.052562	0.001109	300	4	301	7	310	48
6c	3851	579	147	0.038225	0.000497	0.274122	0.006833	0.052012	0.001025	242	3	246	5	286	45
6	2444	707	97	0.039966	0.000523	0.285294	0.005460	0.051773	0.000643	253	3	255	4	275	29
7	1320	1613	77	0.047035	0.000626	0.334875	0.007167	0.051637	0.000784	296	4	293	5	269	35
8	853	743	46	0.046957	0.000641	0.340777	0.009719	0.052634	0.001232	296	4	298	7	313	53
9	795	826	45	0.048419	0.000660	0.360732	0.006500	0.054034	0.000551	305	4	313	5	372	23
10	396	126	20	0.046426	0.000674	0.328450	0.011061	0.051311	0.001469	293	4	288	8	255	66
11	866	720	47	0.047585	0.000648	0.338498	0.008788	0.051593	0.001056	300	4	296	7	267	47
12	475	298	24	0.044740	0.000643	0.333302	0.012929	0.054031	0.001852	282	4	292	10	372	77
Schönbachwald gneiss (14; rhyolitic tuff)															
1	694	189	32	0.046822	0.000726	0.338396	0.008506	0.052417	0.000940	295	7	296	12	304	41
2	1700	1067	81	0.044103	0.000656	0.309817	0.007997	0.050949	0.000984	278	7	274	8	239	45
3	769	69	32	0.043890	0.000677	0.314381	0.007034	0.051951	0.000748	277	7	278	12	283	33
4	1433	365	62	0.044006	0.000659	0.307693	0.008541	0.050711	0.001095	278	7	272	8	228	50
5	2251	31	83	0.039945	0.000590	0.295888	0.006631	0.053723	0.000812	252	6	263	7	359	34
6	564	198	24	0.041583	0.000671	0.309796	0.015980	0.054032	0.002540	263	7	274	13	372	106
7	526	228	26	0.046552	0.000742	0.331394	0.010585	0.051630	0.001330	293	7	291	15	269	59
8	848	837	44	0.044038	0.000693	0.328526	0.014277	0.054105	0.002088	278	7	288	12	375	87
9	704	216	24	0.031525	0.000502	0.209663	0.007492	0.048235	0.001450	200	5	193	16	111	67
10	1191	271	51	0.043080	0.000653	0.303485	0.010519	0.051093	0.001499	272	7	269	10	245	68
11	1330	544	63	0.045691	0.000686	0.330454	0.009103	0.052454	0.001117	288	7	290	9	305	49
12	2964	1323	90	0.027195	0.000408	0.184129	0.004785	0.049105	0.000955	173	4	172	9	153	45
13	510	179	22	0.041708	0.000479	0.296089	0.014967	0.051488	0.002462	263	3	263	12	263	110
Granatspitz Central Gneiss (15; intrusive granite)															
1	916	278	39	0.042734	0.000448	0.299484	0.008015	0.050827	0.001187	270	3	266	6	233	54
2	1146	437	86	0.073910	0.000741	0.563828	0.008448	0.055327	0.000550	460	4	454	5	425	22
3c	352	31	25	0.074070	0.000829	0.567408	0.010838	0.055559	0.000786	461	5	456	7	435	31
3	1168	49	66	0.060825	0.000612	0.452211	0.006187	0.053921	0.000437	381	4	379	4	368	18
4c	278	112	12	0.040050	0.000500	0.276101	0.010797	0.050000	0.001777	253	3	248	9	195	82
4r	4875	77	146	0.032874	0.000318	0.233205	0.002962	0.051451	0.000365	209	2	213	2	261	16
5	1044	377	55	0.035866	0.000424	0.249143	0.025445	0.050381	0.005037	227	3	226	21	213	217
6	320	33	22	0.072221	0.000816	0.545037	0.011016	0.054735	0.000843	450	5	442	7	401	35

Table 2 (*Contd.*)

Grain	$U_{(ppm)}$	$Th_{(ppm)}$	$Pb_{(ppm)}$	Calculated ratios						Calculated ages in Ma ($\pm 1\ \sigma$)					
				$^{206}Pb/^{238}U$	($\pm 1\ \sigma$)	$^{207}Pb/^{235}U$	($\pm 1\sigma$)	$^{207}Pb/^{206}Pb$	($\pm 1\ \sigma$)	$^{206}Pb/^{238}U$		$^{207}Pb/^{235}U$		$^{207}Pb/^{206}Pb$	
7c	2269	165	90	0.042792	0.000421	0.305311	0.004432	0.051747	0.000492	270	3	271	3	274	22
7r	199	116	10	0.041050	0.000645	0.258310	0.040244	0.045638	0.006985	259	4	233	32	0	36
8	824	407	42	0.042390	0.000447	0.305328	0.008275	0.052239	0.001238	268	3	271	6	296	54
9	323	163	14	0.038757	0.000481	0.256855	0.015955	0.048066	0.002852	245	3	232	13	103	134
10	353	111	15	0.042842	0.000511	0.313398	0.014116	0.053055	0.002227	270	3	277	11	331	95
11	159	112	9	0.043016	0.000625	0.318311	0.022154	0.053668	0.003557	272	4	281	17	357	150
12	1434	117	57	0.042716	0.000432	0.308562	0.005267	0.052390	0.000657	270	3	273	4	303	29

centre and overgrowth zones form a single, coherent population plotting analytically concordant (Fig. 7a). The mean $^{206}Pb/^{238}U$ and $^{207}Pb/^{235}U$ age of 300 ± 5 Ma ($\chi^2 = 1.13$ and 0.84 respectively) may indicate the magmatic crystallization age due to no excess scatter. The younger ages of analyses 9 and 10 may be explained by the high uranium contents of 1820–1954 ppm compared with the range of 476–1542 ppm in the other zircons. These high U contents caused more intense metamictization. SHRIMP spot 12 has unintentionally been placed on a disturbed zone as evidenced in the CL image (Fig. 4f, grain 10).

Heuschartenkopf gneiss (12; rhyolitic tuff)

Fifteen grains have been measured. Thirteen zircons have analytically concordant $^{206}Pb/^{238}U$, $^{207}Pb/^{235}U$ and $^{206}Pb/^{207}Pb$ ratios, yielding an extrusion age of the rhyolitic precursor of 299 ± 4 Ma ($^{206}Pb/^{238}U$; $\chi^2 = 0.46$) (Fig. 7b). Two SHRIMP spots (4, 12) are slightly discordant and younger. Spot 4 is situated on a non-luminescent, high-U centre zone (Fig. 4g), which probably led to the observed rejuvenation. Analyses 12 is from a homogeneous centre of a long-prismatic zircon, and the cause of the isotopic disturbance is not apparent.

Venediger Central Gneiss (13; intrusive tonalite)

Seven analyses from 12 grains are analytically concordant with a mean $^{206}Pb/^{238}U$ and $^{207}Pb/^{235}U$ age of 296 ± 4 Ma ($\chi^2 = 0.88$) and 296 ± 5 Ma ($\chi^2 = 0.45$) respectively (Fig. 7c). That age is interpreted to represent the intrusion age of the gneiss precursor. Five analyses are slightly discordant with significantly lower $^{206}Pb/^{238}U$ ratios and high U contents up to 7149 ppm (spots 1, 4, 5, 6, 6c). These analyses may be aligned on a regression line towards zero. Given the positive correlation of U content and discordancy, these analyses are interpreted to reflect rejuvenation due to metamictization. Two further analyses (2, 9) reveal an older component, although no cores can be seen within the CL images (Fig. 4c). Adding these two analyses to the seven concordant analyses would increase the mean ages to 299 ± 5 Ma ($\chi^2 = 1.71$) and 301 ± 7 Ma ($\chi^2 = 1.20$) respectively.

Schönbachwald gneiss (14; rhyolitic tuff)

Ten analyses from 13 grains yield an analytically concordant mean $^{206}Pb/^{238}U$ age of 279 ± 5 Ma (with some excess scatter as indicated by $\chi^2 = 4.72$) and a $^{207}Pb/^{235}U$ age of 280 ± 7 Ma ($\chi^2 = 1.51$). These age data are interpreted as the extrusion age of the rhyolitic precursor of the muscovite gneiss (Fig. 8a). The other three analyses are younger, two of them (5, 12) due to Pb loss associated with high U content. The other one (9) obviously reveals a disturbed U/Pb system, yet is interpreted as being derived from the main population.

Granatspitz Central Gneiss (15; intrusive granite)

Sixteen SHRIMP spots have been placed on 13 grains. Eight analyses from the centre, intermediate and rim positions form a single, coherent population that is slightly discordant (Fig. 8b). Thus, the mean $^{206}Pb/^{238}U$ age of 268 ± 3 Ma ($\chi^2 = 0.99$) is interpreted as minimum crystallization age, whereas the real age may be slightly older. In the rest of this paper the somewhat arbitrary mean $^{207}Pb/^{235}U$ age of 271 ± 4 Ma ($\chi^2 = 0.37$) is chosen to represent the intrusion age, although any age between 265 Ma (lower age limit of the mean $^{206}Pb/^{238}Pb$ age) and 275 Ma (upper age limit of the mean $^{207}Pb/^{235}Pb$ age) would be statistically equivalent. The age range is within error limits similar to a Rb–Sr whole rock age of 265 ± 39 Ma (Cliff 1977).

Three analyses (9, 5, 4r) have lower $^{206}Pb/^{238}U$ ratios. The lowest ratio from a rim zone (4r) may be explained by an unusually high U content of 4875 ppm U, which probably caused a high degree of radiation damage, and, in consequence, radiogenic Pb loss. The other two analyses derived from zircons, which are unusually densely filled with inclusions (9) or metamict (5). We tentatively associate both cases with radiogenic Pb loss and rejuvenation. Three further spots from centre regions (2, 3c, 6) yield a concordant age of 457 ± 16 Ma (mean $^{206}Pb/^{238}U$ age) and a fourth spot from a rounded intermediate zone (3) of 381 ± 4 Ma

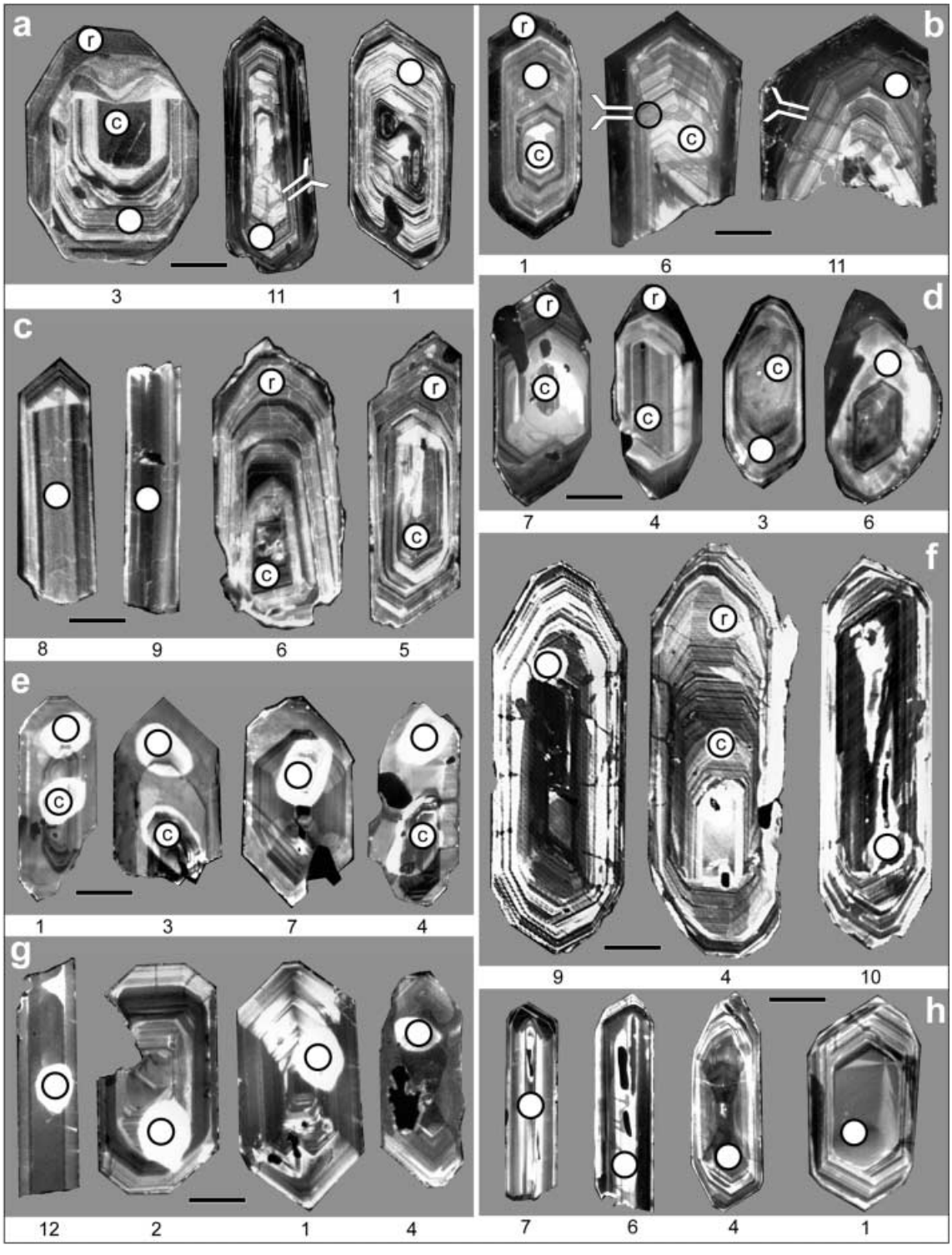

Fig. 4 CL images of zircons from Variscan granitoids (**a–d**) and volcanics (**e–h**); *black circles* indicate SHRIMP spot size and position; *grain numbers* as in Table 2; *scale bars* 35 μm; *r* rim; *c* centre; intermediate position without letter. **a** Hochweißenfeld gneiss: corrosion phenomena and leached cracks (*Y*) are frequent and similar to the Augengneiss of Felbertauern. **b** Augengneiss of Felbertauern: due to intense deformation, many zircons are broken and reveal surface corrosions and cracks (*Y*). **c** Venediger Central Gneiss: some grains show centres of a chaotic mosaic (*6*). Extremely elongated grains have their pyramidal tips broken off, which caused a parallel-striped appearance of the oscillatory zones (*9*). **d** Granatspitz Central Gneiss. **e** Falkenbachlappen gneiss. **f** Peitingalm gneiss: some grains reveal cracks vertical to their *c*-axis (probably due to their largeness) (*9*). **g** Heuschartenkopf gneiss: the zircons reveal two different shapes – a small, short-prismatic, oscillatory-zoned variant (*1*) and a long-prismatic, parallel-zoned variant with broken-off pyramidal tips (*12*). **h** Schönbachwald gneiss

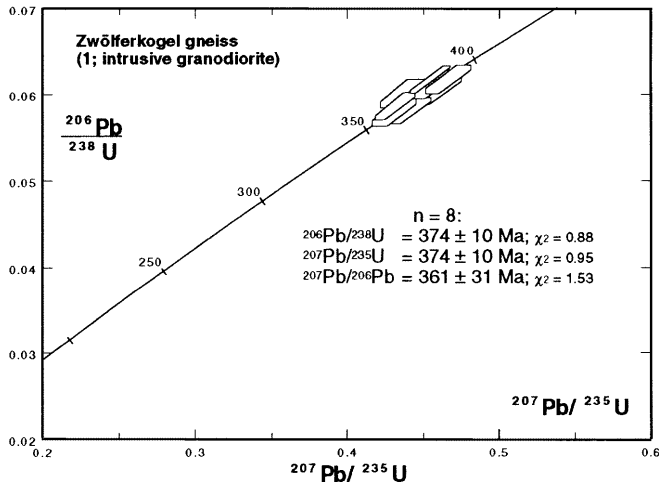

Fig. 5 Concordia plot showing SHRIMP analyses for zircons from a Middle Devonian (Givetian) leucocratic gneiss

(Fig. 4d). These centre regions are interpreted as inherited zircon cores; their age of ca. 460 Ma may possibly mark the age of the source rock, from which the Granatspitz magma was derived. The existence of inherited cores may explain the unsuccessful dating attempt with conventional isotope dilution technique of Cliff (1981), where three zircon fractions yield almost concordant $^{206}Pb/^{238}U$ ages of 264–278 Ma and $^{207}Pb/^{235}U$ ages of 269–281 Ma, corroborating our data, yet one fraction pointed to an U/Pb age older than 325 Ma.

Discussion

The U/Pb SHRIMP ages of eight Variscan leucocratic orthogneisses reveal close temporal relationships between granitoid intrusions and volcano-sedimentary deposits during three distinct periods in the Early Carboniferous (Visean), Late Carboniferous (Stephanian) and Early Permian. A further age indicates a pulse of magmatic activity as early as Middle Devonian.

Middle Devonian (Givetian) and Early Carboniferous (Visean)

Amalgamation of the northward-drifting northern portions of the "Intra-Alpine" terrane hosting the Tauern Window area with Laurussia–Avalonia probably did not occur prior to the Late Devonian, as may be judged from the primitive volcanic-arc chemistry of the 374 ± 10-Ma-old Zwölferkogel granodioritic gneiss (Fig. 9, inset map). This rock appears to be another representative of the Early Variscan, potentially subduction-related I-type granitoid group as defined by Finger et al. (1997). Regarding age and chemistry, it is particular similar to the so-called Cetic granitoid suite (Frasl and Finger 1988), which consists of exotic boul-

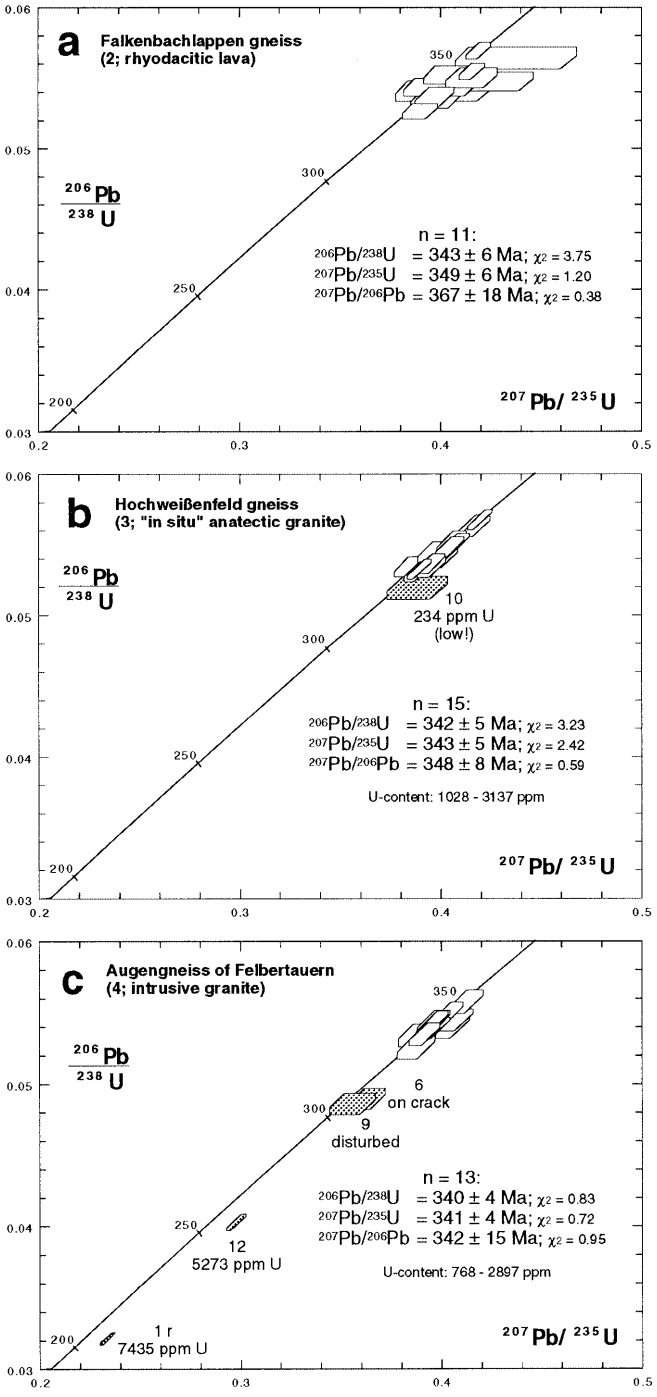

Fig. 6a–c Concordia plots showing SHRIMP analyses for zircons from Early Carboniferous (Visean) leucocratic gneisses. *Grey polygons* are rejuvenated main population zircons that have suffered Pb loss

ders of sodium-rich, Hbl-bearing tonalites to granodiorites with very primitive Sr-isotope characteristics embedded in the northern Alpine flysch (Finger et al. 1997).

A further, important occurrence of Middle to Late Devonian I-type plutons is in the northern realm of the Armorican terrane, the Mid-German Crystalline High.

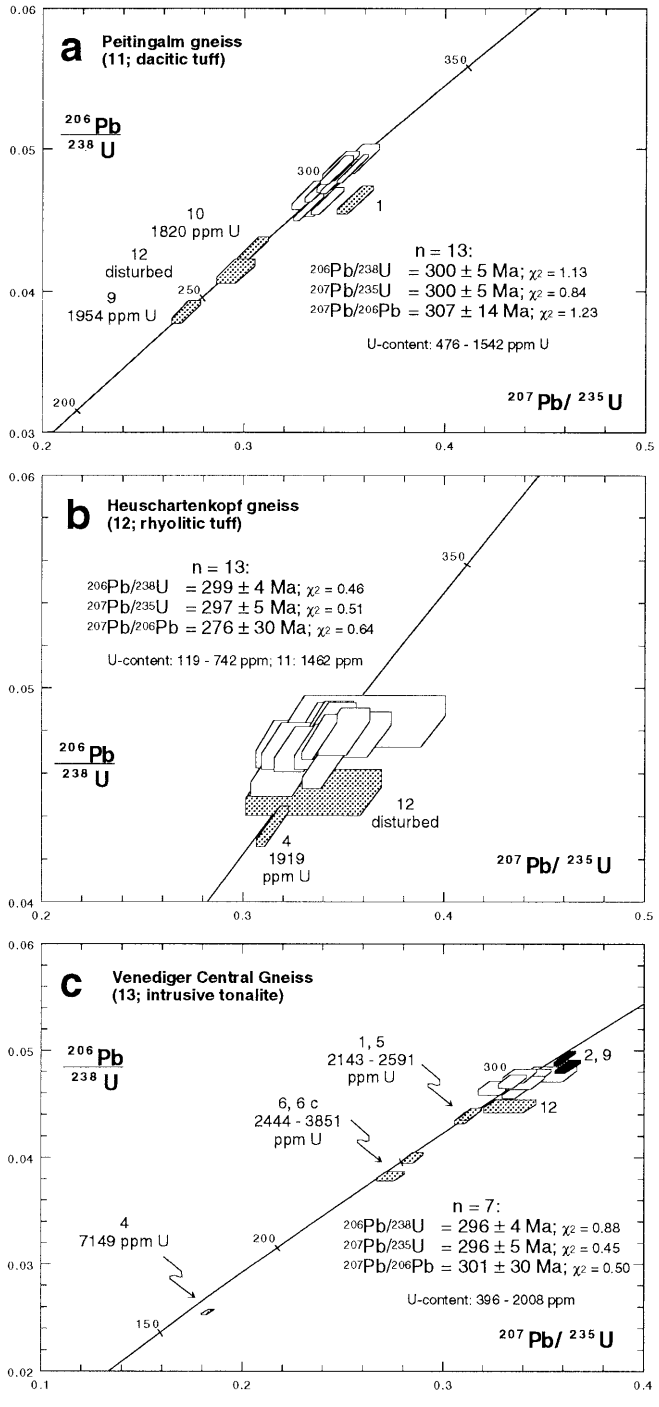

Fig. 7a–c Concordia plots showing SHRIMP analyses for zircons from Late Carboniferous (Stephanian) leucocratic gneisses. *Black polygons* indicate inherited zircons; *grey polygons* are rejuvenated main population zircons that have suffered Pb loss

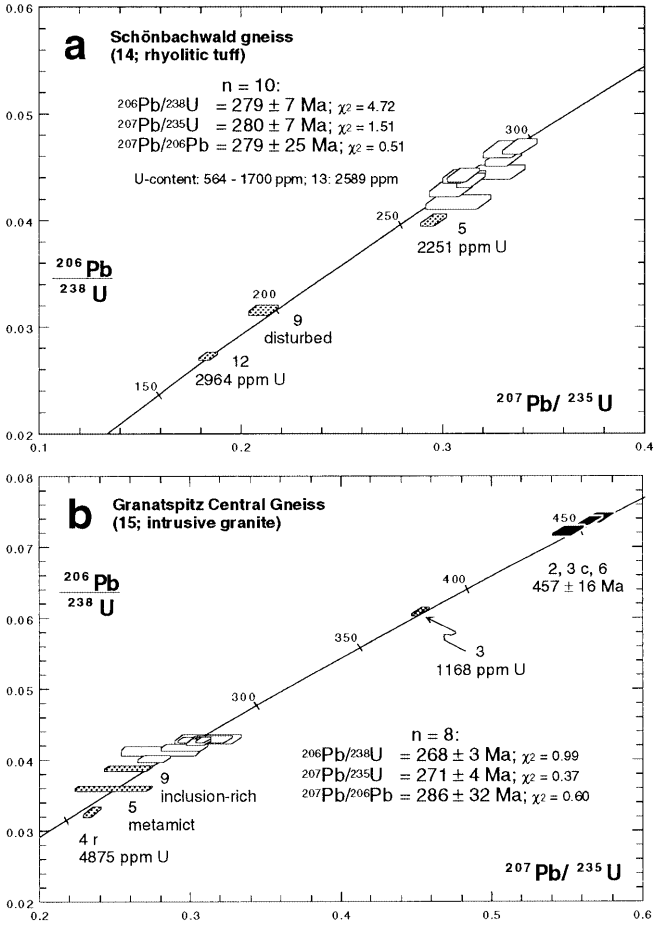

Fig. 8a–b Concordia plots showing SHRIMP analytical points for zircons from Permian leucocratic gneisses. *Black polygons* indicate inherited zircons; *grey polygons* are rejuvenated main population zircons that have suffered Pb loss

That granitoid belt can be traced westwards by boreholes in the Paris basin and is usually correlated with a "Normannian High" concealed under the English Channel (Holder and Leveridge 1986). The rocks have geochemical signatures of volcanic-arc type settings and include a few gabbros (Odenwald: 362 ± 7 Ma; Kirsch et al. 1988), diorites, tonalites and large masses of normal and high-K granodiorites (Schwarzburg anticline: ca. 370 Ma; Gehmlich et al. 1997). Granitoids of similar type and age have also been recorded in the Central Bohemian Batholith of the Moldanubian zone (Kosler et al. 1993; Janousek et al. 1995; Holub et al. 1997).

From the foregoing, it is likely that the collision between the Tauern Window basement and Laurussia–Avalonia occurred between the Late Devonian and the Early Carboniferous. Roughly 340-Ma-old "in situ" anatexites (e.g. Hochweißenfeld gneiss: 342 ± 5 Ma) adjacent to thrust planes and Variscan amphibolite-facies metamorphism up to some 325 Ma (Pestal 1983) indicate already deeply buried segments of stacked nappes. The collisional events are documented in 340–334-Ma-old high-K granites (e.g. Augengneiss of Felbertauern: 340 ± 4 Ma; Knorrkogel gneiss: 334 ± 8 Ma; Table 1) accompanied by volcanic activity in a syn-collisional extension setting (e.g. Falkenbachlappen gneiss: 343 ± 6 Ma). Obviously, intra-montane transtensional basins containing detrital sediments and calc-alkaline volcanics (or plutons and dykes at somewhat deeper levels) evolved during the Visean, despite a

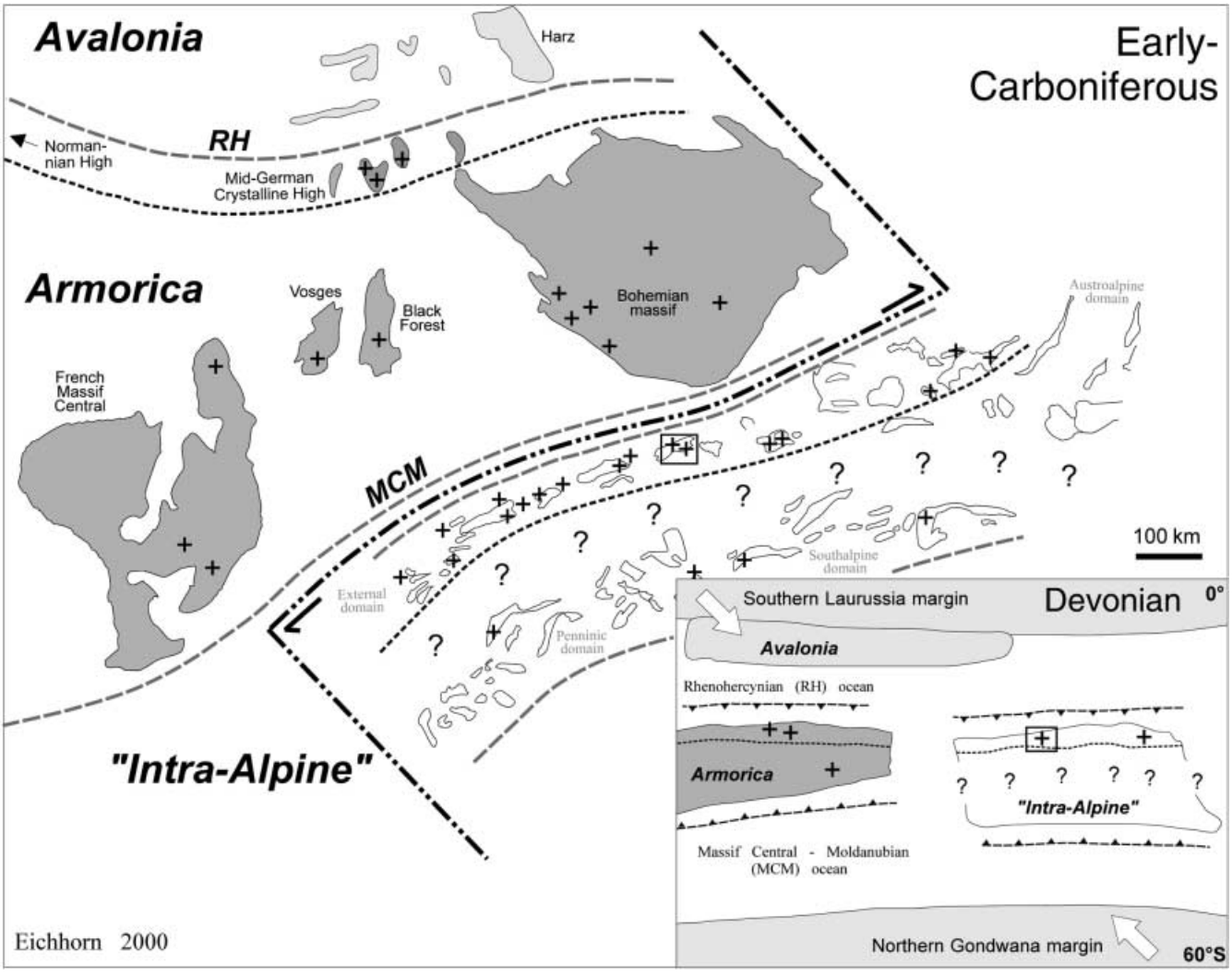

Fig. 9 Tentative palinspastic reconstruction of central Europe in the Late Carboniferous period (modified after Franke et al. 1995; Finger et al. 1997; Tait et al. 1997; Raumer 1998). Large-scale dextral strike-slip movements are assumed to have moved the ''Intra-Alpine'' terrane from a easterly position to a southerly position relative to Armorica. Thus, the Devonian and Early Carboniferous granitoid intrusions (marked by *crosses*) in the northernmost parts of the Armorican (Mid-German Crystalline High) and ''Intra-Alpine'' terrane may have resulted from the same processes, i.e. the southward subduction of a Rhenohercynian (RH) ocean, and their subsequent collision with Laurussia–Avalonia. *Framed areas* mark the approximate position of the Tauern Window area

compressional/transpressional regime prevailing on a large scale. The magmatic evolution of the Tauern Window area at that time is similar to the evolution reported from the ''External domain'' (Switzerland): Intramontane basins containing sub-aerial clastic sediments and pyroclastic tuffs were probably formed between 345 and 335 Ma and were filled in under an extensional setting (Schaltegger and Corfu 1995). Simultaneously, high-K magmas intruded and thermal metamorphic peak conditions prevailed at 337–333 Ma in deeper levels (data compilation in Raumer 1998).

Bearing in mind the Late Carboniferous dextral westward wrenching of Gondwana relative to Laurussia (Arthaud and Matte 1977), dextral mega-strike-slip movements may have shifted the ''Intra-Alpine'' terrane to the south of Armorica. Prior to that, the ''Intra-Alpine'' terrane may have been located in an south-eastward extension of Armorica. Accordingly, the Devonian Zwölferkogel gneiss and the Cetic granitoids may be related to a southward subduction of the Rhenohercynian ocean (Fig. 9, inset map).

Since subduction probably ceased in the Late Devonian (Franke et al. 1995), an active Andean-type margin setting is an unlikely explanation for the Early Carboniferous magma pulse. Schaltegger (1997) proposed that these magmas may have been generated during a short phase of decompressional melting of lithospheric mantle and lower crustal sources. This melting stage may have been triggered by detachment of the subducted oceanic slab or simply by thermal erosion of the Variscan orogenic root through a convecting mantle. An extensional tectonic regime for the emplacement of the granitoids is also suggested by their partly shallow intrusion into coeval volcano-sedimentary basin sequences.

A possible mechanism for producing the Visean "in situ" anatexites (e.g. Hochweißenfeld gneiss) may be inferred from their conjectured position at the base of major thrust planes. Quartzo-feldspathic amphibolite-facies rocks (e.g. pre-Variscan biotite–plagioclase gneisses and banded amphibolites of the Old Gneiss Series) positioned near the base of a thick nappe pile may have started to melt due to local shear heating and the potential addition of water released from overridden rocks (e.g. paragneisses of the Old Gneiss Series). Therefore, the 340 Ma formation time of the anatexites may indirectly date the process of Variscan nappe-stacking. However, it must be emphasized that the S-type Granatspitz Central Gneiss, which has previously also been attributed to the oldest generation of Variscan granitoids and regarded as an indicator for Early Carboniferous crustal anatexis (Finger et al. 1993, 1997; Schermaier 1993), is much younger (Early Permian). The mechanisms to generate the huge mass of the Permian Granatspitz magma by regional crustal anatexis are independent from the Early Carboniferous processes discussed before.

Late Carboniferous (Stephanian)

We conjecture from the lack of geochronological data in the time span 340–300 Ma that the central Tauern Window area experienced a period of magmatic quiescence combined with uplift and erosion as evidenced in the Habach syncline: There, an equivalent to the Augengneiss of Felbertauern (340 ± 4 Ma), dated by Vavra and Hansen (1991) at ca. 334 Ma, was uplifted and eroded, until volcanic eruptions at 299 ± 4 (Heuschartenkopf gneiss) and 300 ± 5 Ma (Peitingalm gneiss), and again at 279 ± 7 Ma (Schönbachwald gneiss). This produced the unconformable deposition of pyroclastics, tuffites and tuffs near the volcanic centre and of carbonate-rich psammitic to pelitic sediments further off. In addition, the same granite has been intruded by huge masses of I-type, calc-alkaline granodiorites and granites ("Tux Augen- and Flaser-gneisses"). The emplacement time of the granodiorites and granites is bracketed by the age of tonalites equivalent to the Venediger tonalite (i.e. 296 ± 4 Ma), into which they also intruded according to Schermaier (1993), and the 292 ± 6 Ma age of aplitic injections ("Reichenspitze" granites) post-dating the granodiorites and granites. The latter age is a recalculated Rb–Sr whole rock isochron age (Finger et al. 1993) that uses data of Besang et al. (1968). The estimated intrusion time of the granodiorites and granites between 296 and 292 Ma is only marginally younger than the deposition time of ca. 300 Ma of the pyroclastics, tuffites and tuffs unconformably overlying the Early Carboniferous granite.

Further evidence for magmatic quiescence and uplift can be inferred from the Venediger nappe, which consists of pre-Variscan Stubach Group equivalents (Old Gneiss Series) and of Variscan gneiss lamellae. During the Variscan orogeny, these rocks were probably nappe-stacked with the gneiss precursors adjacent to major thrust planes. They exhibit a nebulous, diffuse contact with the much older surrounding migmatites and have been partly generated by "in situ" anatexis (Finger et al. 1993) at 342 ± 5 Ma (Hochweißenfeld gneiss) and 334 ± 8 Ma (Knorrkogel gneiss; Finger and Quadt 1993). About 40 Ma later, these originally deep-seated rocks had to be uplifted and cooled significantly to explain the sharp, discordant contacts of cross-cutting granodioritic to granitic dykes and minor intrusive bodies derived from the Venediger magmatic suite (296 ± 4 Ma) (Schermaier 1991). The uplift was presumably accompanied by erosion and sedimentation, as indicated by the deposition of Late Carboniferous to Early Permian clastic sediments (now micaschists) on pre-Variscan Stubach Group equivalents (Franz et al. 1991).

The similarities of this evolution in the Tauern Window area to the evolution of the External domain in the Western Alps (Schaltegger and Corfu 1992, 1995; Bussy and Raumer 1994; Sergeev et al. 1995; Schaltegger 1997) are obvious: There, a basin and a reactivated successor basin are reported: 303 ± 4 to 299 ± 2-Ma-old pyroclastics rest unconformably on 345–335-Ma-old sediments and tuffs. They are intruded by an intermediate, high-K calc-alkaline sill at 310 ± 3 Ma (Westphalian) as well as by an acid, high-K calc-alkaline to subalkaline granite at 298 ± 2 Ma (Stephanian). Schaltegger and Corfu (1995) did not favour a rapid sequence of volcanic deposition, burial and intrusion during the Stephanian. They assumed a caldera collapse and the subsequent intrusion of 298 Ma old magma into the overlying volcanics. In the central Tauern Window, 310-Ma-old granitoids are missing or still undetected. However, such Westphalian magmatic activity has been detected in the eastern Tauern Window, where tonalites and granodiorites have been emplaced at 314 ± 7 Ma and 313 ± 10 Ma respectively (Cliff 1981).

The Stephanian volcano-sedimentary deposits and voluminous Venediger and Tux granitoid suites bear dominantly crustal isotopic and volcanic-arc geochemical signatures (Finger et al. 1993). Schaltegger and Corfu (1995) and Schaltegger (1997) proposed for the External domain that the Stephanian magmatism was a consequence of post-orogenic uplift and adiabatic decompression unrelated to subduction zones. They based their conclusions on the numerous transtensional basins, beginning to evolve or being reactivated during the Stephanian. Schaltegger and Corfu (1995) further argued that the observed calc-alkaline character of these granites is no direct evidence for active subduction of oceanic crust. It may simply be the result of a mixture of previously subducted oceanic lithosphere, which was underplated or incorporated into the lower continental lithosphere and crustal melts. Such melts may have been generated by heat supplied by upwelling, hot (asthenospheric) mantle.

On the contrary, subduction-zone related models for that time have been proposed for the Tauern Window

area: Finger and Steyrer (1990) envisaged melting or dehydration of remnant oceanic crust beneath the collision zone. This may have been triggered by further descent of the slab after a presumed detachment from the overlying orogen. A similar mechanism has been proposed for the Visean high-K calc-alkaline magmatic series by Schaltegger (1997). Finger and Steyrer (1990) and Finger et al. (1997) postulated an Andean-type active margin with subduction of oceanic crust under the southern edge of Laurussia. Considering the Late Carboniferous oblique wrenching of Gondwana relative to Laurussia with the opening of the Paleotethys gulf, it is possible that transpressional–transtensional tectonics persisted in more western parts of the Variscan orogen (e.g. External domain), whilst, at the same time, Paleotethys oceanic crust was already being subducted further to the east (e.g. Tauern Window area).

Our data cannot corroborate or disprove one of the above models. However, the existence of various Stephanian volcano-sedimentary troughs of intra-continental character, previously unknown in the Tauern Window area, the lack of evidence for a 300-Ma-old ocean in that area, and the similarities of the Tauern Window and External domain magmatic evolutions are tentatively used as arguments. Thus the production of Stephanian melts in the Tauern Window was probably guided by magmatic underplating and crustal decompressional melting combined with post-orogenic crustal extension, and not by subduction-related processes.

Early Permian

Stephanian sedimentary troughs in the External domain have been interpreted as successor basins of older (Visean) basins (Schaltegger and Corfu 1995; Raumer 1998). That evolutionary model has not been accepted for the central Tauern Window area. However, there is evidence from the Habach syncline (e.g. Schönbachwald gneiss: 279 ± 7 Ma), the Falkenbachlappen syncline (e.g. 283 ± 11 Ma; Loth et al. 1997), and the Porphyrmaterialschiefer synclinal anticline (e.g. 284 + 2/−3 Ma; Söllner et al. 1991) that old (Visean?) basins existed and have been reactivated or continued to exist until the Early Permian. The plutonic equivalents of the Permian volcanics may be represented by the 271 ± 4-Ma-old S-type Granatspitz Central Gneiss. That age is almost identical to an age of 267 ± 4 Ma reported from a major A-type granite body in the eastern Tauern Window (Quadt et al. 1999).

The Permian magmatic activity, which is prominent in the Tauern Window and yet to be reported from the External domain, has been identified as subalkaline to alkaline granitoids and rhyolites in the Penninic, Austroalpine and Southalpine domains (Schaltegger 1997). The late-stage Variscan S- and A-type granites with Permian intrusion ages may be associated with local extension along continental wrench zones that were running through the Variscan orogenic crust (Schaltegger 1997) or with a Permian rifting event heralding the start of the Alpine orogeny (Quadt et al. 1999).

Conclusions

Four pulses of granitoid melt generation in the Middle Devonian, Early Carboniferous, Late Carboniferous and Permian are documented in the central Tauern Window, each representing a distinct stage in the evolution of the Variscan collisional orogeny. It evolved through (1) Andean-type active plate margin setting (≥370 Ma), (2) remnant subduction zone activation (ca. 340 Ma), (3) decompressional melting (≈280–300 Ma), and (4) the beginning of intra-continental rifting (< 280 Ma). The Variscan Carboniferous magmatic evolution of the Tauern Window area is similar to the evolution reported from the more westerly Aar, Aiguilles Rouges and Mont Blanc massifs of the External domain. This fact supports the paleogeographic interpretation of the Tauern Window as an eastward extension of the External domain (Lammerer 1988; Raumer 1998).

A close temporal relationship between these plutonic pulses and the deposition of volcano-sedimentary strata can be documented for the first time in the Tauern Window: an older sequence of Visean lavas and tuffs intercalated with a few sedimentary layers, which formed at 343 ± 6 Ma, is analogous to the pyroclastic tuffs and clastic sediments of the External domain (Aar massif; Switzerland). A younger, 300 ± 5 Ma explosive volcanic series is characterized by felsic to intermediate lavas, tuffs and tuffites intercalated by mafic lapilli-tuffs and tuffaceous breccias. A third period of volcanic activity at about 279 ± 7 Ma produced felsic tuffs embedded in micaschists and phyllites. Such Early Carboniferous (Visean), Late Carboniferous (Stephanian) and Permian volcano-sedimentary sequences were probably deposited in intra-continental troughs during periods of transtension, which had been interrupted by periods of convergence (transpression) and/or uplift and erosion. Apparently, the Tauern Window region repeatedly experienced periods of magmatic quiescence, erosion and uplift. Several kilometres of upper crust must have been eroded from Early Carboniferous to Late Carboniferous/Permian times, as documented in the Habach syncline.

Concerning the paleogeographic position of the Tauern Window in the Variscan Fold Belt, an eastward continuation of the northernmost part of the Armorican terrane (Mid-German Crystalline High) is considered possible.

Acknowledgements We would like to thank R. Huber, R. Jünger, M. Kupferschmied, P. Schauder and U. Teipel (Institut für Allgemeine und Angewandte Geologie; Ludwig-Maximilians-Universität München) for providing some of the zircon samples. Zircon preparation and morphological investigation was likewise done at that institute. CL imaging was undertaken in Munich and at the Electron Microscopic Centre (University of Western Australia) in

Perth. Zircon analyses were carried out on the sensitive high-resolution ion microprobe spectrometer (SHRIMP II) at Perth during two measurement campaigns of R.E. and G.L. in February/March 1997 and August 1998. SHRIMP II is operated by a consortium consisting of the Curtin University of Technology, the University of Western Australia and the Geological Survey of Western Australia, with the support of the Australian Research Council. We gratefully acknowledge financial support of the Albert-Maucher-Stiftung (Munich), the Deutsche Forschungsgemeinschaft (DFG; Ho 488/23-1) and the Austrian Science Foundation (grant no. 9434). We are indebted to R. Cliff and an unknown reviewer for their critical and constructive comments.

References

Arthoud F, Matte P (1977) Late Paleozoic strike-slip faulting in southern Europe and northern Africa: result of a right-lateral shear zone between Appalachians and the Urals. Bull Geol Soc Am 88: 1305–1320

Beil F (1986) Petrographischer Bestand, Genese und Alter der ''Porphyrmaterialschiefer'' am Nordrand des Tauernfensters zwischen Hintertux und Gerlospaß. PhD Thesis, Univ Münster

Beil-Grzegorczyk F (1988) Petrographie, Genese und stratigraphische Stellung des ''Porphyrmaterialschiefers'' am Nordrand des Tauernfensters zwischen Hintertux und Gerlospaß. Jahrb Geol Bundesanst Wien 133: 219–230

Besang C, Harre W, Karl F, Kreuzer H, Lenz H, Müller R, Wendt I (1968) Radiometrische Altersbestimmungen (Rb/Sr und K/Ar) an Gesteinen des Venediger-Gebietes (Hohe Tauern, Österreich). Geol Jahrb 86: 835–844

Bussy F, Raumer JF von (1994) U–Pb geochronology of Palaeozoic magmatic events in the Mont-Blanc crystalline massif, western Alps. Schweiz Mineral Petrogr Mitt (Abstr) 74: 514–515

Claoue-Long JC, Compston W, Roberts J, Fanning CM (1995) Two Carboniferous ages: a comparison of SHRIMP zircon dating with conventional zircon ages and $^{40}Ar/^{39}Ar$ analyses. Soc Sed Geol Spec Publ 54: 3–21

Cliff RA (1977) Rb–Sr measurements on granite-gneisses from the Granatspitzkern, Hohe Tauern, Austria. Verh Geol Bundesanst Wien 1977: 101–104

Cliff RA (1981) Pre-Alpine history of the Penninic zone in the Tauern Window, Austria: U–Pb and Rb–Sr geochronology. Contrib Mineral Petrol 77: 262–266

Compston W, Williams IS, Meyer C (1984) U–Pb geochronology of zircons from lunar breccia 73217 using a sensitive high-resolution ion-microprobe. J Geophys Res 89: 525–534

Eichhorn R (1995) Isotopengeochemische und geochronologische Untersuchungen an Gesteinen und Mineralen der Scheelit-Lagerstätte Felbertal (Land Salzburg, Österreich). Münchner Geol Hefte 15: 1–78

Eichhorn R, Schärer U, Höll R (1995) Age and evolution of scheelite-hosting rocks in the Felbertal deposit (Eastern Alps): U–Pb geochronology of zircon and titanite. Contrib Mineral Petrol 119: 377–386

Eichhorn R, Höll R, Jagoutz E, Schärer U (1997) Dating scheelite stages: a strontium, neodymium, lead approach from the Felbertal tungsten deposit, Central Alps, Austria. Geochim Cosmochim Acta 61: 5005–5022

Eichhorn R, Höll R, Loth G, Kennedy A (1999) Implications of U–Pb SHRIMP zircon data on the age and evolution of the Felbertal tungsten deposit (Tauern Window, Austria). Int J Earth Sci 88: 496–512

Finger F, Quadt A von (1993) Genauere U/Pb Alter für Granite und Granitgneise durch sorgfältige Zirkonselektion unter dem Durchlichtmikroskop – Der Knorrkogelgneis der Hohen Tauern als Beispiel. Ber Dtsch Min Ges 5: 118 (Abstr)

Finger F, Steyrer HP (1988) Granite-types in the Hohe Tauern (Eastern Alps, Austria) – some aspects on their correlation to Variscan plate tectonic processes. Geodyn Acta 2: 75–87

Finger F, Steyrer HP (1990) I-type granitoids as indicators of a late Paleozoic convergent ocean/continent margin along the southern flank of the Central European Variscan orogen. Geology 18: 1207–1210

Finger F, Kraiger H, Steyrer HP (1985) Zur Geochemie des K1-Gneises der Scheelitlagerstätte Felbertal (Pinzgau/Salzburg) – ein Vorbericht. Karinthin 92: 225–235

Finger F, Frasl G, Haunschmid B, Lettner H, Quadt A von, Schermaier A, Schindlmayr AO, Steyrer HP (1993) The Zentralgneise of the Tauern Window (Eastern Alps): insight into an Intra-Alpine Variscan batholith. In: Raumer JF von, Neubauer F (eds) Pre-Mesozoic geology in the Alps. Springer, Berlin Heidelberg New York, pp 375–391

Finger F, Roberts MP, Haunschmid B, Schermaier A, Steyrer HP (1997) Variscan granitoids of Central Europe: their typology, potential sources and tectonothermal relations. Mineral Petrol 61: 67–96

Franke W, Dallmeyer RD, Weber K (1995) Geodynamic evolution. In: Dallmeyer RD, Franke W, Weber K (eds) Pre-Permian geology of central and eastern Europe. Springer, Berlin Heidelberg New York, pp 579–593

Franz G, Mosbrugger V, Menge R (1991) Carbo-Permian pteridophyll leaf fragments from an amphibolite facies basement, Tauern Window, Austria. Terra Res 3: 137–141

Frasl G (1958) Zur Seriengliederung der Schieferhülle in den Mittleren Hohen Tauern. Jahrb Geol Bundesanst Wien 101: 323–472

Frasl G, Finger F (1988) The ''Cetic Massif'' below the Eastern Alps – characterized by its granitoids. Schweiz Mineral Petrogr Mitt 68: 433–439

Frasl G, Frank W (1966) Einführung in die Petrographie und Geologie des Penninikums im Tauernfenster. Aufschluß 15: 30–58

Fuchs G (1958) Beitrag zur Kenntnis der Geologie des Gebietes Granatspitze–Großvenediger (Hohe Tauern). Jahrb Geol Bundesanst Wien 101: 201–248

Gehmlich M, Tichomirowa M, Linnemann U (1997) Datierung von magmatischen Zeitmarken in der saxothuringischen Zone mittels Einzelzirkon-Evaporationsmethode (abstr). Schr Dtsch Geol Ges 2: 52

Gradstein FM, Ogg J (1996) A Phanerozoic time scale. Episodes 19/1,2: 3–5

Gritz W (1996) Geochemie ausgewählter granitoider Gesteine aus dem zentralen Teil des Tauernfensters (Osttirol). Jahrb Geol Bundesanst Wien 139: 29–34

Höck V, Kraiger H, Lettner H (1993) Oceanic vs continental origin of the Paleozoic Habach Formation in the vicinity of the Felbertal scheelite deposit (Hohe Tauern, Austria): A geochemical approach. Abh Geol Bundesanst Wien 49: 79–95

Holder MT, Leveridge BE (1986) Correlation of the Rhenohercynian Variscides. J Geol Soc Lond 143: 141–147

Höll R (1975) Die Scheelitlagerstätte Felbertal und der Vergleich mit anderen Scheelitvorkommen in den Ostalpen. Bayer Akad Wiss, Math Naturwiss Kl 157a: 1–114

Holub FV, Rossi P, Cocherie A (1997) Radiometric dating of granitic rocks from the Central Bohemian Plutonic Complex (Czech Republic): constraints on the chronology of the thermal and tectonic events along the Moldanubian–Barrandian boundary. CR Acad Sci Paris 325: 19–26

Janousek V, Rogers G, Bowes DR (1995) Sr–Nd isotopic constraints on the petrogenesis of the Central Bohemian Pluton, Czech Republic. Geol Rundsch 84: 520–534

Jünger R, Teipel U, Höll R (1999) Geochemistry of Variscan metavolcanics in the Falkenbachlappen (Central Tauern Window). 89th Annu Meet Geol Vereinigung ''Old crust – new problems''. Terra Nostra 99/1: 115 (abstr)

Kirsch H, Kober B, Lippolt HJ (1988) Age of intrusion and rapid cooling of the Frankenstein gabbro (Odenwald, SW-Germany) evidenced by $^{40}Ar/^{39}Ar$ and single zircon $^{207}Pb/^{206}Pb$ measurements. Geol Rundsch 77: 693–711

Kosler J, Aftalion M, Bowes DR (1993) Mid–late Devonian plutonic activity in the Bohemian Massif: U–Pb zircon isotopic

evidence from Stare Sedlo and Mirotice gneiss complex, Czech Republic. Neues Jahrb Mineral Abh 9: 417–431
Kraiger H (1989) Die Habachformation – ein Produkt ozeanischer und kontinentaler Kruste. Mitt Österr Geol Ges 81: 47–64
Kupferschmied MP (1993) Structural studies in the Western Habach Group (Tauern Window, Salzburg, Austria). Abh Geol Bundesanst Wien 49: 67–78
Kupferschmied MP (1994) Geologische Untersuchungen im Tauernfenster zwischen Hollersbachtal und Krimmler Achental. Münchner Geol Hefte 12: 1–160
Kupferschmied MP, Höll R (1994) Die geologische Neuaufnahme der Habachmulde und ihre genetischen Implikationen für die Habachgruppe (Tauernfenster/Ostalpen). Jahrb Geol Bundesanst Wien 137: 139–153
Kupferschmied MP, Höll R, Miller H (1994) Lithologische und strukturgeologische Untersuchungen in der Krimmler Gneiswalze (Tauernfenster/Ostalpen) und ihrem Umfeld. Jahrb Geol Bundesanst Wien 137: 155–170
Lammerer B (1986) Das Authochthon im westlichen Tauernfenster. Jahrb Geol Bundesanst Wien 129: 51–67
Lammerer B (1988) Thrust-regime and transpression-regime tectonics in the Tauern window. Geol Rundsch 71: 143–156
Lammerer B, Weger M (1998) Footwall uplift in an orogenic wedge: the Tauern Window in the Eastern Alps of Europe. Tectonophysics 285: 213–230
Loth G, Höll R (1996) Zirkonmorphologische und geochemische Untersuchungen von Gesteinen aus der Stubachgruppe (Tauernfenster, Österreich) In: Amann G, Handler R, Kurz W, Steyrer HP (eds) 6. Symposium Tektonik–Strukturgeologie–Kristallingeologie: Erweiterte Kurzfassungen (abstr). Facultas, Salzburg, pp 261–264
Loth G, Eichhorn R, Höll R, Kennedy A (1997) Age and evolution of the Stubach Group (Tauern Window, Eastern Alps): U–Pb–SHRIMP results of zircons from several gneiss types. Ber Dtsch Min Ges 9: 230 (abstr)
Ludwig KR (1991) A plotting and regression program for radiogenic isotope data. Version 2.53. US Geol Surv Open-File Rep 91
Oehlke M, Weger M, Lammerer B (1993) The ''Hochfeiler Duplex'' – imbrication tectonics in the SW Tauern Window. Abh Geol Bundesanst Wien 49: 107–124
Peindl P, Höck V (1993) U/Pb and $^{207/206}$Pb-dating of zircons from the Habach-Formation (Central Tauern Window, Austria) (abstr). Terra Nova 5 (suppl 1): 392–393
Pestal G (1983) Beitrag zur Kenntnis der Geologie in den mittleren Hohen Tauern im Bereich des Amer- und des Felbertales. PhD Thesis, Univ Wien
Pidgeon RT (1997) Gem zircon: a new role as a standard for the measurement of geological time using ion microprobes. Z Dtsch Gemmol Ges 46/1: 21–28
Quadt A von, Haunschmid B, Finger F (1999) Mid-Permian A-type plutonism in the eastern Tauern Window. Ber Dtsch Min Ges11: 185 (abstr)
Raith M, Mehrens C, Thöle W (1980) Gliederung, tektonischer Bau und metamorphe Entwicklung der penninischen Serien im südlichen Venediger-Gebiet, Osttirol. Jahrb Geol Bundesanst Wien 123: 1–37
Raumer JF von (1998) The Paleozoic evolution in the Alps: from Gondwana to Pangea. Geol Rundsch 87: 407–435
Schaltegger U (1997) The age of an Upper Carboniferous/Lower Permian sedimentary basin and its hinterland as constrained by U–Pb dating of volcanic and detrital zircons (northern Switzerland). Schweiz Mineral Petrogr Mitt 77: 101–111
Schaltegger U, Corfu F (1992) The age and source of Late Hercynian magmatism in the Central Alps: evidence from precise U–Pb ages and initial Hf isotopes. Contrib Mineral Petrol 111: 329–344
Schaltegger U, Corfu F (1995) Late Variscan ''basin and range'' magmatism and tectonics in the Central Alps: evidence from U–Pb geochronology. Geodinam Acta 8: 82–98
Schermaier A (1991) Geologischpetrographische Untersuchungen zur präalpidischen Entwicklung am Ostrand des Venedigermassivs (Hohe Tauern). Jahrb Geol Bundesanst Wien 134: 345–367
Schermaier A (1993) Gliederung der Zentralgneise im mittleren und westlichen Tauernfenster: Geologie – Petrographie – Zirkontypologie – Geochemie. PhD Thesis, Univ Salzburg
Schmidegg O (1961) Geologische Übersicht der Venedigergruppe. Verh Geol Bundesanst Wien 1961: 34–55
Schumacher ME, Laubscher HP (1996) 3D crustal architecture of the Alps–Appenines join: a new view on seismic data. Tectonophysics 260: 349–363
Sengl F (1991) Geologie und Tektonik der Schönachmulde (Zillertaler Alpen, Tirol). PhD Thesis, Univ München
Sergeev SA, Meier M, Steiger RH (1995) Improving the resolution of single-grain U/Pb dating by use of zircon extracted from feldspar: application to the Variscan magmatic cycle in the Central Alps. Earth Planet Sci Lett 134: 37–51
Söllner F, Höll R, Miller H (1991) U–Pb-Systematik der Zirkone in Meta-Vulkaniten (''Porphyroiden'') aus der Nördlichen Grauwackenzone und dem Tauernfenster (Ostalpen, Österreich). Z Dtsch Geol Ges 142: 285–299
Steiger RH, Jäger E (1977) Subcommission on Geochronology Convention on the use of decay constants in Geo- and Cosmochronology. Earth Planet Sci Lett 36: 359–362
Steyrer HP (1982) Geochemie, Petrographie und Geologie der Habachformation im Original gebiet zwischen äußerem Habachtal und Untersulzbachtal (Pinzgau, Salzburg). PhD Thesis, Univ Salzburg
Steyrer HP (1983) Die Habachformation der Typlokalität zwischen äußerem Habachtal und Untersulzbachtal (Pinzgau/Salzburg). Mitt Österr Geol Ges 76: 69–100
Steyrer HP, Höck V (1985) Geochemistry of the metabasites in the Habach Formation (Salzburg, Hohe Tauern, Austria): a preliminary report. Ophioliti 10: 441–455
Tait JA, Bachtadse V, Franke W, Soffel HC (1997) Geodynamic evolution of the European Variscan fold belt: palaeomagnetic and geological constraints. Geol Rundsch 86: 585–598
Teipel U, Höll R (2000) Lamprophyrische, dacitische und andesitische Ganggesteine im Felbertal und Amertal (mittlere Hohe Tauern): Petrographie und Geochemie. Neues Jahrb Geol Paläont Monatsh (in press)
Thiele O (1974) Tektonische Gliederung der Tauernschieferhülle zwischen Krimml und Mayrhofen. Jahrb Geol Bundesanst Wien 117: 55–74
Tollmann A (1975) Ozeanische Kruste im Pennin des Tauernfensters und die Neugliederung des Deckenbaus der Hohen Tauern. Neues Jahrb Geol Palaeont Abh 148(3): 286–319
Vavra G (1989) Die Entwicklung des penninischen Grundgebirges im östlichen und zentralen Tauernfenster der Ostalpen. Geochemie, Zirkonmorphologie, U/Pb-Radiometrie. Tübinger Geowiss Arb A6: 1–150
Vavra G, Hansen BT (1991) Cathodoluminescence studies and U/Pb-dating of zircons in pre-Mesozoic gneisses of the Tauern Window: implications for the Penninic basement evolution. Geol Rundsch 80: 703–715
Weger M (1998) Duktile Kinematik kontinentaler Kruste am Beispiel der Zentralgneise des westlichen Tauernfensters (Ostalpen, Österreich und Italien). Münchner Geol Hefte A22: 1–268
Williams IS, Buick IS, Cartwright I (1996) An extended episode of early Mesoproterozoic metamorphic fluid flow in the Reynolds range, central Australia. J Metamorph Geol 14: 29–47
Winkler M (1996) Genese und geodynamische Stellung der Zentralgneise im Tauernfenster. Tübinger Geowiss Arb A30: 1–116